C/302

R

Argonne National Laboratory

REACTOR DEVELOPMENT PROGRAM
PROGRESS REPORT

August 1961

302

9-28-61

DISCLAIMER

DISCLAIMER

Portions of this document may be illegible in electronic image products. Images are produced from the best available original document.

ARGONNE NATIONAL LABORATORY
9700 South Cass Avenue
Argonne, Illinois

REACTOR DEVELOPMENT PROGRAM
PROGRESS REPORT

August 1961

N. Hilberry, Laboratory Director

Division	Director
Chemical Engineering	S. Lawroski
Idaho	M. Novick
Metallurgy	F. G. Foote
Reactor Engineering	B. I. Spinrad
Remote Control	R. C. Goertz

- - - - -

Report coordinated by R. M. Adams

Issued September 15, 1961

FOREWORD

The Reactor Development Program Progress Report, issued monthly, is intended to be a means of reporting those items of significant technical progress which have occurred in both the specific reactor projects and the general engineering research and development programs. The report is organized in a way which, it is hoped, gives the clearest, most logical over-all view of progress. The budget classification is followed only in broad outline, and no attempt is made to report separately on each sub-activity number. Further, since the intent is to report only items of significant progress, not all activities are reported each month. In order to issue this report as soon as possible after the end of the month editorial work must necessarily be limited. Also, since this is an informal progress report, the results and data presented should be understood to be preliminary and subject to change unless otherwise stated.

The issuance of these reports is not intended to constitute publication in any sense of the word. Final results either will be submitted for publication in regular professional journals or will be published in the form of ANL topical reports.

The last six reports issued
in this series are:

January 1961	ANL-6307
February 1961	ANL-6328
March 1961	ANL-6343
April 1961	ANL-6355
May 1961	ANL-6374
June 1961	ANL-6387

TABLE OF CONTENTS

TABLE OF CONTENTS

TABLE OF CONTENTS

I. WATER COOLED REACTORS (040101)

A. EBWR

1. 100-Mw Modifications - Reboilers

The Struthers-Wells Corporation has notified the Laboratory that it cannot meet the schedule previously submitted for delivery of the reboilers. On August 8 a new schedule was submitted which predicts completion of the first reboiler by September 30, and the second by October 10, 1961.

The original scheduled delivery of both reboilers was August 31. This delay is very disappointing and will set back the startup of EBWR. It was hoped to obtain experience in the operation of the air-cooled heat exchangers prior to the coming of freezing weather. The air-cooled heat exchangers will be operated before supplying steam to the Laboratory heating system to master their control and to eliminate "bugs," and to assure that no leakage exists between the tube side and the shell side of the primary heat exchangers.

However, it now appears that it will be necessary to perform the shakedown operation of the air-cooled heat exchangers under adverse weather conditions. This condition involves a calculated risk since the danger of freezing up tubes must be faced until experience provides performance data to determine proper operating conditions.

2. Core I-A

a. <u>Storage Rack</u> - Some difficulty was experienced in welding Boral sheet and in tack welding the material after assembly. All exposed edges of the boral sheet have been given two coats of an epoxy resin. The storage rack is now complete and is being prepared for installation.

b. <u>Zircaloy-2 Follower Control Rods</u> - Corrosion testing of a 10-in. Zircaloy-2 cross was completed. Indications of corrosion products near the spot welds persist. The fusion welds at the end of the crosses have been completed and the crosses will be riveted to the Type 304 stainless steel transition. After the units are riveted, they will be corrosion tested in a large autoclave.

A vendor has been found with suitable facilities for heat treating the 10-in. poison crosses. One such cross was shipped and Laboratory personnel will witness the heat treatment.

3. Reactor Operation

     a.   EBWR Steam Quality Studies - Steam quality studies using radioactive sodium tracer have been conducted on EBWR with the new high shroud. Effects of feedwater ring location in the downcomer, and of reactor pressure and power have been evaluated. Steam quality has exceeded 99.98% in all cases (entrainment less than 0.02% based on weight of steam) up to 20-Mwt power level at 300 psig.

     b.   EBWR Turbine - Some noises still exist in the governor end of the turbine after a two-week down time for repairs. The pedestal end was taken apart for further investigation.

     c.   EBWR Operator Training - Most of the operators have had experience in starting up the reactor within the past several weeks. This phase of the program should be completed within the next month.

4. AMU-ANL-EBWR Summer Study Group

     The eight-week summer study group on the EBWR was completed August 11. Participants consisted of staff members from five Associated Midwest Universities plus an additional twelve representatives of power companies from both the United States and abroad.

     The course of study consisted in part of four weeks of lectures presented by members of the Laboratory's staff. Texts for the four weeks of lectures were ANL and TID documents on subjects related to EBWR design, development, and operation. Copies of approximately 35 different technical documents were given out.

     The final four-week period was organized to permit the university staff participants to conduct individual investigation and study under the guidance of Laboratory staff members. This work was conducted in areas of interest where the work could conveniently be continued at the university either independently or in conjunction with nuclear development activities at ANL on the EBWR. Response to this program by the AMU Summer Study Advisory Committee, as well as the AMU staff participants, has been very gratifying.

5. Core II

     Bids have been received for the fabrication of fuel rods for Core II, and are in the process of evaluation.

6. Reactor Decontamination

     The reactor decontamination program consists of two principal efforts. The first is to evaluate the spread of fission product activity through the steam section of a boiling water reactor in the event of a

fuel element failure. A stainless steel loop which simulates the action of a boiling water reactor is being used to study the behavior of fission products present in the circulating water. Fission products are introduced into the loop by allowing the heated water to corrode irradiated natural uranium metal. Sample strips which are inserted in the vapor space of the system provide the samples for post-run evaluation of fission product distribution and deposition. The second effort is to determine adequate methods for removing the deposited activity.

In a sixteen-day loop run at 200 psi pressure and a steam velocity of 0.8 ft/sec, steam disengaging factors varied from 1.3×10^3 for ruthenium to 2×10^4 for barium-lanthanum. Analysis of activity deposited on the metal strips in the loop indicated that the predominant activities deposited were cerium, ruthenium and zirconium. Extrapolation of this deposition data was made using data on the activity content of the Dresden reactor core as a reference in order to estimate the radiation levels. The radiation level in a six-inch steam line was calculated to be 8.5 and 11.6 mr/hr, respectively, for ruthenium-103 and zirconium-95, the predominant activities deposited.

Laboratory investigations have continued the examination of the peroxide-oxalate reagent as a decontaminant. Current experiments indicated poor decontamination of specimens contaminated in the vapor space of the loop in contrast to the excellent decontamination previously obtained with samples contaminated in the laboratory. Corrosion tests at 90°C indicated a penetration rate of approximately 0.05 mil per hour for the low chromium steels exposed to a solution of 0.50 $\underline{M}$ sodium oxalate, 3 $\underline{M}$ hydrogen peroxide, 1 $\underline{M}$ acetic acid, 0.175 M sodium acetate. Reduction of the temperature to 60°C resulted in tenfold decrease in the corrosion rate.

B. BORAX V

1. Installation of Reactor and Components

All three core structures (boiling core structure, central superheater core structure, and peripheral superheater core structure) have been re-assembled and successfully test-fitted, with and without the forced-convection baffle in place, in the reactor vessel. Figure 1 shows these items. In each case the reactor vessel head was installed and measurements were taken to determine the size of spacers required on top of the core structure struts to give the proper deflection on the Belleville Spring. As a result of test installations, the guide dowels in the bottom of the reactor vessel were modified and guide funnels were attached on the bottom of two core structure legs to facilitate future remote installations. Minor modifications to core structure handling tools and storage stands have also been made. Figure 2 shows the central superheater core structure in the reactor vessel.
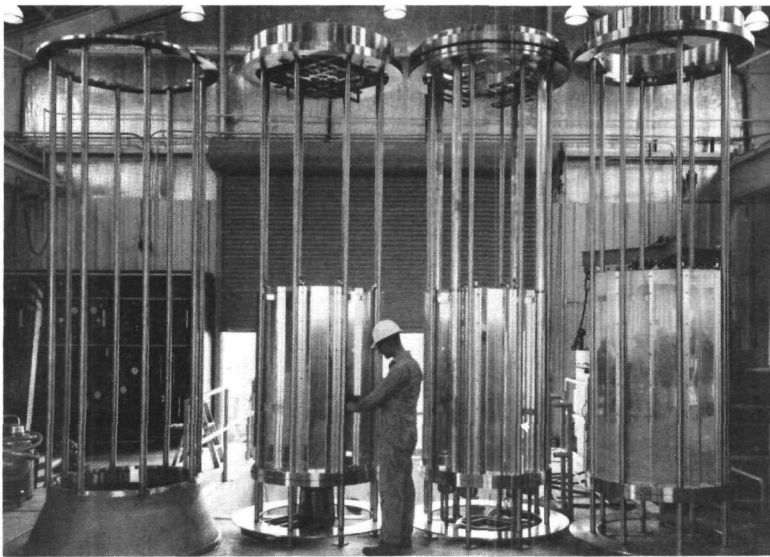
Figure 1

Left to right: Forced Convection Baffle, Central Superheater Core Structure, Peripheral Superheater Core Structure, and Boiling Core Structure.

Figure 2

Central Superheater Core Structure in Reactor Vessel. Flexible Superheated Steam Manifolds and Belleville Spring Assembly in place.
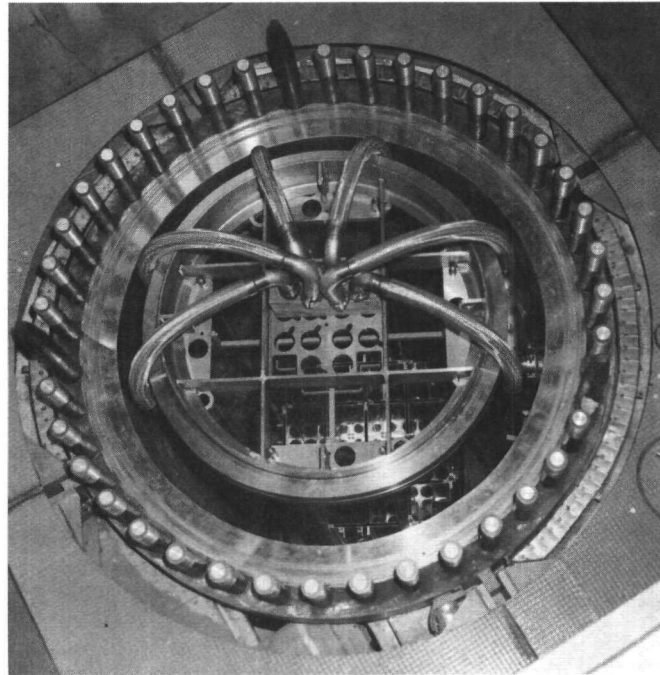
The nine thermal sleeve assemblies in the control rod nozzle shield plugs were modified, after test-fitting, to correct the orientation of two of them and double the strength of the Inconel-X wave spring in the bayonet joint of all. These plugs have now been permanently installed. The saturated steam collector and the two feedwater spargers are being modified to facilitate proper alignment and ease of remote handling.

The following additional reactor vessel internals have been successfully test-fitted: control-rod-channel orifice plates, poison addition nozzle, four blank caps for superheated-steam outlet nozzles, flexible superheated

steam outlet manifolds for both central and peripheral superheater cores, and the flood-and-drain manifold extension downcomers for both superheating cores.

Test-fitting of the reactor vessel extension spool was satisfactory, but indicated that a second, larger spool is required for installing and removing the feedwater spargers, superheated steam flexible manifolds and downcomer instrumentation.

Installation of all nine complete control-rod-drive assemblies, the seal-water supply and leakoff tubing, the seal housing blowdown piping, and the motor drive assemblies is completed. Installation of new change gears and dust covers on the motor drive assemblies was finished. Wiring of the rod drive motors, selsyns and controls is complete and checkout has begun. The rod drives and seals must be removed again before operation to install new 17-4 PH control rod extension shafts and to connect the control rods. Figure 3 shows the control rod drive installation.
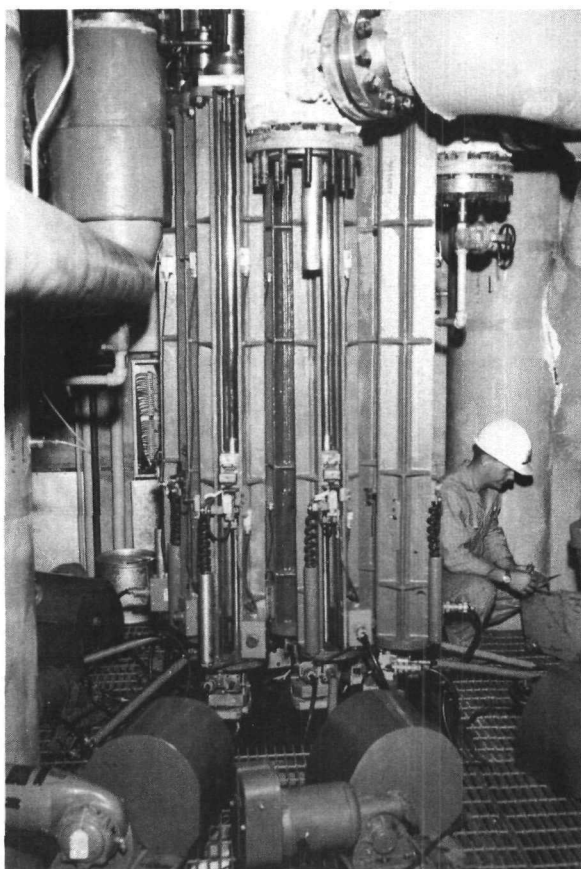
Figure 3

View of Sub-reactor Room. Nine Control Rod Drive-Seal Assemblies in Place. Motor Drive Assemblies Being Installed.

Connecting of sampling lines to the reactor system is complete except for the upper and lower reactor water and steam dome sampling points. The water chemistry sampling station has been connected to the sampling

lines and is ready to hydro-test. A major portion of the wiring for sampling system pumps and instruments is completed. Installation work and painting in the auxiliary chemistry laboratory is essentially complete.

Cables were pulled for all conductivity cells and radiation monitors, except those in the turbine building. Audible monitors for remotely listening to the operation of control rod drives, dash pot, and the forced-convection pump have been installed and are operational. Alarm and interlock limit-switches have been installed on the manually-operated flood valve and turbine trip-actuator. New wiring and fixtures have been installed for better lighting in the subreactor room and access shaft.

Calibration of repiped transmitters in the process instrumentation system continued. Damage to two units was traced to excessive current flowing through the bellows-to-transmitter linkage when the instrument piping was welded. Cause of this was the manufacturer's improper electrical bonding between the meter body and transmitter while using the building frame as an electrical return for the welding machine. The shield wall temperature alarm has been remounted and is being rewired. Checkout and debugging of other instrument, control, and alarm circuits continues.

All nuclear instrumentation is operational except the period circuits, which have not yet been tested to determine the effect of noise from plant electrical equipment.

All manually-operated valves have been checked for freedom of operation and packing gland adjustment. Temporary cleanup screens have been installed in the suction lines of the condensate pumps, feed pumps, and auxiliary pump in preparation for startup.

2. Procurement and Fabrication

a. <u>Superheat Fuel Elements</u> - Inspection of the second group of evaluation plates fabricated by AI, six type HPD (half peripheral depleted) and six type FCD (full central depleted) fuel plates, was completed. Nondestructive and destructive tests showed that these 12 plates met the specifications. Although isolated dimensional measurements were out of specifications, the vast majority of measurements were within tolerances and the plates as a whole were acceptable.

An additional 38 type FCD plates containing depleted UO_2 have been received from AI. These plates are to be used for assembly development. Nondestructive tests only were performed on these plates. Approximately 80% of the plates failed to pass the squareness tests, but were acceptable on all other nondestructive tests.

All fixtures required for brazing superheater fuel assemblies have been fabricated. Development of the spot-welding technique for holding longitudinal spacer wires to the fuel plates during the brazing operation is proceeding.

b. Reactor Components - Four additional stainless-steel-clad Boral sections of control rods are being fabricated as spares and as replacements for rods which failed in the autoclave tests.

Twenty boiling fuel assembly boxes have been completed. Completion of the remainder is delayed by slow delivery of lower grids from the vendor. The demister-type steam dryer, for use with the central superheater, has been finished. Special hold-down boxes and chimneys for use with instrumented fuel assemblies are 50% complete. Planning and procurement necessary for the fabrication of the instrumented boiling and superheater fuel assemblies continues. A technique of fabricating the 17-4 PH control rod extension shafts with no straightening operation has been successfully demonstrated. Installation of brackets and clips was completed to enable remote handling of all in-vessel temperature-compensating couplings. The five cruciform and four tee-shaped orifice plates for the control rod channels in the core structure shrouds were completed.

Fabrication of components for the remodeled fuel transfer coffin has started. A depleted uranium extension section for the coffin has been received. Fabrication has started on a right-angle-drive socket wrench for the temperature-compensating couplings on the superheated steam manifolds, a special lifting sling for the Belleville Spring, and a reactor vessel dust cover.

Procurement of components and materials of the differential pressure probe and Staucheibe tube downcomer instrumentation systems has been initiated.

c. Plant Components - Modification of the lower forced-convection-pump bearing housing has been started to correct excessive pumping of lubricating oil. These modifications were specified by the manufacturer.

Material for the blowdown filter system has been procured. Fabrication of the reactor-vessel-nut storage racks, the control rod storage racks, and installation of the new seal water control system for the forced-convection pump are awaiting delivery of material and components.

Invitations to bid on a contract to perform certain piping insulation repairs and additions, have been released. Preliminary proposals have been invited on a combination seal water and hydrostatic test pump.

A purchase order has been placed for a high-pressure, high-temperature sampling system pump to be located in the subreactor room. Bids have been invited on a new resin charge to restore the rated capacity of the makeup-water demineralizer.

A new control valve has been ordered to replace the defective raw water supply valve to the makeup-water demineralizer and a new stop valve has been ordered for the reactor vent line.

d. <u>Experimental Equipment</u> - Fabrication of the aluminum liner, tank and fuel racks and the steel track and supporting structure for installation in the AFSR thermal column is essentially complete. This equipment will be used for checking out the cadmium-ratio void measurement technique proposed for use on BORAX-V.

3. Design

Detailed design of the differential pressure probes and Staucheibe tube systems for installation on the reactor vessel downcomer has been completed. D/P cells which have a range of 4 to 20 in. of H_2O will be used to measure the differential pressures. Detailed design of the duplex flux-wire counting machine was essentially completed. Arrangement drawings of in-vessel instrumentation system components in the upper reactor pit and west trench are nearing completion. Detailed design of the modifications to the fuel-handling coffin to permit "head-off" reloading have been finished and design of the coffin modification and tool to permit reloading of boiling fuel assemblies through nozzles in the reactor vessel head continues. Detailed design of a second, larger reactor vessel extension spool has started. It will provide better access around the reactor top.

Detailed design of the in-vessel portion of the rotating oscillating rod assembly is nearing completion. Engineering design of the pressure seal and variable speed drive for this unit continues.

Calculations made to date for control rod worth have employed the PDQ code and the application of a logarithmic derivative condition at control rod surfaces. The value of ϕ'/ϕ was obtained by graphical analysis of the fluxes given by transport theory solutions, wherein the thin regions adjacent to the control rods are explicitly stated. Variations of this method developed at ORNL are now being tried. This involves a numerical determination of ϕ'/ϕ from SNG results and is another method of homogenizing for PDQ problems.

The accuracy of the calculational methods used for setting the fuel loadings for BORAX V is being checked against the results of critical assemblies in ZPR-VII using BORAX V boiling fuel rods. Agreement with preliminary results is favorable.

As part of the AEC hazards evaluation on BORAX V, separate on-site reviews and inquires have been held by reactor safety representatives from both COO, and the Division of Licensing and Regulation. In addition, written replies to lists of questions from these organizations have been prepared.

Editing and final typing of the Operating Manual is nearing completion.

4. Development and Testing

a. <u>Control Rods</u> - Of the eighteen stainless-steel-clad Boral sections of control rods which were autoclaved for two weeks in water at 489°F and 600 psig, three were found defective by swelling. Post-mortem investigation has revealed the following: The worst rod had swelled to a thickness of about $\frac{5}{8}$ in., from an original thickness of $\frac{5}{16}$ in., and had a visible leak. The second rod had swelled only about 0.035 in. and after considerable difficulty a tiny leak was finally found in the weld made to seal off the hole in the top of the rod used for helium leak-testing. The third defective rod contained considerable gas pressure and no leak has been found in this rod. An attempt to collect the gas for analysis by drilling a hole in the clad failed. No significant corrosion of the Boral was found in any of the defective rods.

To determine the gas which might be released by degassing of Boral during operation, the total gas content of seven samples of the Boral used in the control rods was determined by melting at 1000°C in a vacuum and collecting and analyzing the gas. The total gas content of the Boral samples varies from 0.02 to 2.24 cc/g of meat. The principal gas was hydrogen, but H_2O, CO_2, CO, CH_4, O_2, A and other gases were also present.

Several of the good rods which passed the autoclave test are being heated in a furnace at 500°F in an attempt to induce outgassing of the Boral. At the end of a week no swelling has been found. To determine the effect of the differential expansion between the stainless steel cladding and Boral, the second defective rod is being thermally cycled from room temperature to 500°F in a furnace. After four cycles there is no evidence of failure of the spot welds in the cladding. A dye penetrant check is being run on all the good rods to look for cracks and pinholes in cladding, spot-welds and edge seal welds. This dye penetrant check will also be used on the four replacement rods which are now being fabricated.

At present the mechanism which caused the failure of 3 rods out of 18 in the autoclave test has not been definitely determined.

It has been decided to perform the following additional fabrication and inspection procedures on all poison sections of the control rods which have passed the autoclave tests.

1.   Redrill helium leak test hole in top of rod and helium leak test again to see if any leaks are present that may have developed in the autoclave, but did not cause failures.

2.   Degas Boral and interior of rod by heating under vacuum in a furnace to maximum temperature which can be sustained without structural damage to rod. (This temperature must be determined by experimenting with samples.)

3.   Put trace amount of He in rod, plug weld to seal the hole in top of rod, and leak-test seal weld.

The four replacement rods which are being fabricated will be helium leak-tested and degassed prior to the autoclave test.

b.   Corrosion Tests - Corrosion tests on samples of Type 304 stainless steel brazed with Coast Metals 60 Alloy have been run in super-heated steam for 85 days at 540°C and 34 days at 650°C, and on samples of Type 304 stainless steel (brazed with NIORA alloy) for 47 days at 540°C and 34 days at 650°C. No significant corrosion has been observed for any of the samples.

c.   In-Core Instrumentation - Development is continuing on the brazing techniques, using NIORA alloy, for installation of stainless steel sheathed thermocouple leads in the boiling fuel thermocouple rods and the seal plate of the pressurized thermal boxes for instrumented fuel assemblies.

An attempt is still being made to develop non-destructive testing techniques to detect flaws in the tantalum-sheathed portions of the boiling fuel rod thermocouples. Eight tantalum-sheated thermocouple samples have been shipped to Thermatest Laboratories, Sunnyvale, California, for testing. Tests will be made in two runs of four thermocouples each. The first group will be used to detect gross failures, and to aid in possible modification of the test run on the second group. Calibration will be attempted on all the samples at temperatures from 100°F to 5000°F, during both heating and cooling cycles.

d.   Plant Tests - The makeup water demineralizer system has been tested and, at rated flow capacity, produces 8 megohm water.

II. SODIUM COOLED REACTORS (040103)

A. General Research and Development

1. ZPR-III

Assembly 35, a mockup of the Fermi reactor (Core B), was constructed in the ZPR-III facility for experimentation. The experimental program has been planned to obtain criticality information for PRDC as well as physics data for this core size and composition. Therefore, the assembly was made a clean core mockup; i.e., the core and blanket regions were assumed to be uniform in composition.

The basic Fermi B reactor will consist of subassemblies containing a UO_2-steel cermet in a 600-liter, cylindrical core region. In the mockup, an eight-drawer sequence containing 7 columns of enriched uranium is used to achieve the proper core composition. Plates of Fe_2O_3 are used to provide the oxygen content, and sodium is present in steel cans.

In the drawers, the core region extends to 18 inches from the front. The average core composition in the 3 drawer sequence is shown in Table I.

Table I. Composition of Core in Eight Drawer Sequence

Material	Density, g/cc	Volume Percent
U^{235}	0.762	4.06
U^{238}	0.057	0.30
Steel	3.91	49.8
O	0.109	4.2
Na	0.287	29.6

For the blanket regions of the assembly, the average Fermi B radial blanket was to be represented. However, material limitations require the use of several blanket types in which depleted uranium and aluminum are used as substitutes for molybdenum, steel and sodium. The blanket regions extend from the approximate radial edge of the core 18 inches, out to a radius of 34 inches and axially 15 inches out from the core. The inner blanket region, about a 3-inch layer adjacent the core, has the composition given in Table II.

Table II. Composition of Radial Fine Blanket

Material	Density, g/cc	Volume Percent
U^{238}	7.49	39.4
U^{235}	0.015	0.8
Molybdenum	0.222	2.2
Steel	1.44	18.3
Sodium	0.268	27.6

It was expected that the assembly would be critical within a 600-liter core size. The blanket was loaded corresponding to a 590-liter core and the approach to critical begun.

The initial core loading contained 222 kg U^{235}, about half the expected critical mass, in the central radial drawers. In the remainder of the drawers, 63 v/o Al replaced the enriched U columns. The approach to critical was made by stepwise substitutions of enriched uranium for the aluminum, building the fuel region out radially. At the 590-liter loading, with 447 kg U^{235}, the assembly was still subcritical. Additional loading was made, substituting core drawers for fine blanket. The final critical mass was 505 kg U^{235} with a core size of 664 liters. Since this volume is beyond the Fermi limitations, the program provided for the addition of a radial nickel reflector to keep the core volume within the 600-liter limitations.

After measuring the worths of fuel and nickel at the edge of the 664-liter core, the fuel loading was reduced to 457.2 kg U^{235} with a 599-liter core. Then another approach to critical was made by stepwise replacement of radial blanket drawers adjacent to the core with nickel reflector drawers. The nickel reflector drawers have the composition given in Table III.

Table III. Composition of Nickel Reflector

Material	Density, g/cc	Volume Percent
Nickel	5.44	61.1
Sodium	0.153	15.8
Steel	0.951	12.1

Criticality was obtained upon loading 104 nickel reflector drawers around the core. It was determined that to be just critical with all rods in, 100.5 nickel drawers were required. This amounts to a layer of nickel reflector around the core radial boundary 2.1 in. thick.

It is estimated that without the nickel reflector, the 600-liter core in the normal radial blanket was subcritical by 1050 inhours, or about 2.5% k. Experiments were run next to determine the worths of different thicknesses and compositions of nickel reflector. The combinations investigated were: (a) one- and two-row-thick layers of 61 volume percent nickel (Table III); (b) one-, two-, and three-row-thicknesses of 71 volume percent nickel (Table IV).

Table IV. Increased Density Nickel Reflector

Material	Density, g/cc	Volume Percent
Nickel	6.36	71.4
Sodium	0.077	7.9
Steel	0.83	10.6

The reflector types were added around only one quarter of the radial core boundary in one half of the reactor. Table V gives the extrapolation of the results to full radial reflection.

Table V.   Worths of Nickel Reflectors*
(Extrapolated to full core)

Nickel, v/o	Average Radial Thickness, in.	Worth	
		inhours	$\Delta k/k$
61	2.08	1050	2.5%
61	2.68	1322	3.2%
61	5.39	1796	4.3%
71	2.68	1470	3.5%
71	5.39	1958	4.7%
71	8.11	2096	5.0%

*With respect to radial fine blanket
composition (see Table II)

Consultation was held with PRDC to determine priority of future experiments with this assembly. PRDC's most important considerations are experiments involving large reactivity effects of channels, end gaps, etc. Experiments are presently under way to measure the reactivity worths of empty sodium channels through the core and axial blankets representative of the Fermi B safety and control rod channels.

2.   ZPR-VI and ZPR-IX

a.   Construction and Procurement - The wireways for the reactor cables have been installed in both cells and the vendor has begun installation of electrical wall cabinets and cell entry cables in one of the cells. The final 6-in. layer of concrete flooring has been poured in both cells. Construction of the supporting frames required for the installation of the reactor tables of ZPR-VI is in progress and the table installation should be accomplished next month.

The remaining four (of eight) reactor matrix support plates have now been received from the supplier. An initial shipment of ZPR-VI and ZPR-IX drawer springs has been received and inspected. The sample shipment of aluminum matrix tubing for ZPR-IX was rejected since the internal dimensions did not meet the specifications.

b.   Leak Testing of Cells - Although the Building D-315 cells have not yet been made leak tight to the point where leak rate tests could be run, sufficient tightness was realized to run the structural pressure tests. Ten psi can be maintained.

The actual structural pressurization tests were conducted by raising the internal pressure 2 psi at a time and reading the corresponding strains. After reaching the maximum pressure of 10 psi, the pressures were reduced at 2 psi steps, thus providing strain readings for the same differential pressures on the way down. The tests extended between approximately 11 p.m. and 6 a.m. as planned. During the intervening seven hours the cell was twice pressurized to 10 psi. Thus, counting readings taken during pressurization and deflation, four strain readings were obtained for each pressure level. Following the replacement of some defective strain gages, the entire test, as described above, was repeated on the eighth night after the first test.

The data are being processed now for comparison with theoretical stresses and strains. Subsequently, extrapolation will be attempted to estimate the ultimate strength of the cell.

B. EBR-I

1. Fabrication of Mark IV Core

The Mark IV core for EBR-I will consist of the following rods:

Fuel Rods	420
Thermocouple Fuel Rods	10
Blanket Rods	120
Thermocouple Blanket Rods	5
Total	555

The fuel rod consists of four plutonium-1.25 w/o aluminum fuel slugs and two depleted uranium blanket slugs. These are NaK bonded in a Zircaloy-2 jacket tube. The fuel slugs are centered in the tube by four full length ribs. Each fuel slug measures 0.232 in. diameter by 2.121-in. long. A hollow Zircaloy spacer and Inconel-X spring are used above the upper blanket slugs.

The jacket tube is 0.300-in. OD. x 0.020-in. wall thickness. It is closed at the lower end by pointed triangular locating fitting. Three 0.049-in. diameter wires are spot welded to the tube to form longitudinal spacer ribs. After loading, a threaded coupling is welded into the top of the tube. NaK is filled through an opening in the top of this coupling. The opening is then plugged and fusion welded.

The ten thermocouple fuel rods are similar to the fuel rods except that the internal components are drilled to receive a Zircaloy-2 thermocouple protector tube.

The blanket rods are similar to the fuel rods except that two additional depleted uranium slugs are used in place of the four plutonium slugs. Five blanket thermocouple rods are required.

Although work was scheduled to begin on the fuel and blanket rods in February, 1961, delivery of satisfactory Zircaloy tubing from the commercial source was delayed. Blanket grade and fuel grade fuel tubing was finally culled from repeated reruns of tubing and the first blanket hardware was received in early May. Development and production ran concurrently, as a result of the delayed receipt of the blanket grade tubing and hardware, and work was completed on the 120 blanket rods during the first week in July.

As of this date, 39 injection cast melts of plutonium-1.25 w/o aluminum core material have been made. A total of 2,019 rough slugs have been cut from 254 castings produced in these melts. Of these, 1,518 slugs have been die coined, heat treated and machined. 1,136 acceptable slugs have been processed and loaded into 284 fuel rods. A total of 196 fuel rods have been welded, bonded, leak detected, eddy current inspected and judged acceptable.

After approximately 800 rough cut slugs were made, the specified slug diameter was reduced by three mils. This required an additional roll sizing operation, upsetting in a new set of dies and remachining. The yield to date of acceptable slugs has averaged approximately 70 percent. This was due to difficulties in producing full length ribs and to three batches of slugs with an abnormally high nickel content which cracked in rolling. Current production yield is averaging over 80 percent.

Fuel grade Zircaloy hardware was not received until late June. Zircaloy tubing is still in short supply and previously rejected hardware is again being culled for additional fuel tubes which may be accepted. Thermocouple rod inserts for 15 thermocouple rods have been received from the vendor. Delivery of stainless steel tube stock for fabrication of extension rods has been promised for late August. Because of these delays it has been necessary to extend the scheduled core delivery date to the last week in September.

C. EBR-II

1. Installation of Equipment - Package 4

a. <u>Cleaning Operations</u> - The cleaning operation is proceeding very satisfactorily. All of the cutting operations for the dismantling of the system have been performed. The cleaning of the lines is about 70% complete. Reinstallation of the piping has not begun.

Significant quantities of undesirable material are being removed by the cleaning procedure. Figure 4 shows the condition in which one of the lines was found. Note the extremely heavy deposit of scale. Figure 5 shows the condition of a 12-inch stainless steel sodium line. The paper is believed to be the remnants of a temporary paper pipe plug used during the welding operation to contain an inert gas atmosphere during the welding of the root pass. This is typical of the type of foreign material which cannot be found by radiographic examination of the piping.
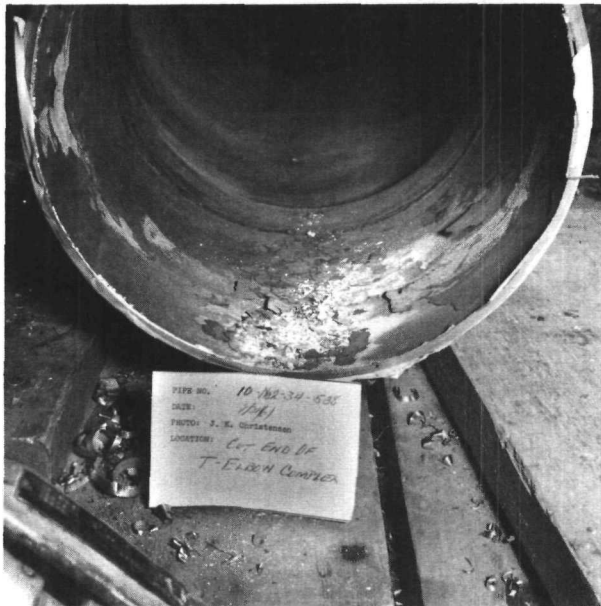
Figure 4. View of Foreign Material Removed from One Line
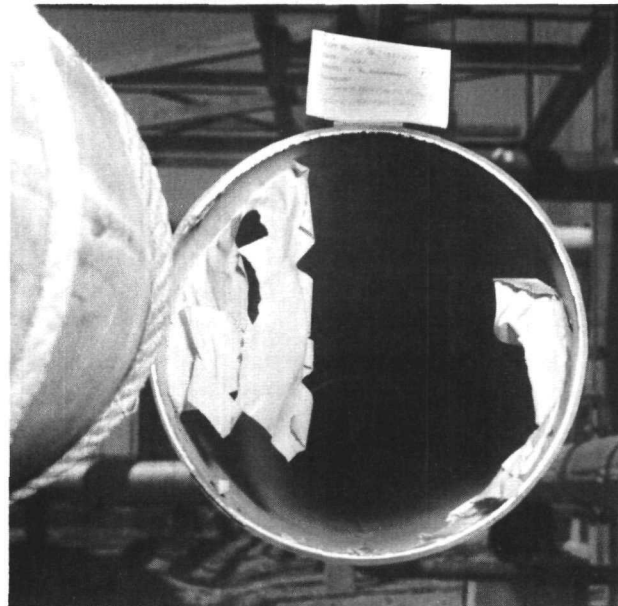
Figure 5. View of 12-inch Stainless Steel Sodium Line with Remnants of Temporary Paper Plug Used during Welding.

The procedure for cleaning the secondary sodium system is described in the Progress Report for July (ANL-6399). Figure 3 of that report shows the procedure for cleaning the evaporator sodium outlet headers. The process consists of propelling an 8-inch cleaning pig through the "S"-shaped 8-inch evaporator sodium outlet line and retrieving it by pushing it through the 10-inch header by a mechanically manipulated 10-inch cleaning pig. Figure 6 shows this 10-inch cleaning pig within the 10-inch header. The wire cable is used for pulling the pig through the line. Since the wire bristles of the brush fit very tightly against the pipe wall, it is necessary to apply considerable force to move it. This is provided by a power operated winch as shown in Figure 7. Figure 8 shows more clearly the cleaning pigs, pipe plug and air attachments, and mechanical winch.

After all the loose material has been removed from the lines by wire brushing with the cleaning pigs, the pipes are wiped clean to remove loose, fine, particulate matter. This is done by using a modified pig with the wire brushes replaced with cloth material. These are shown in Figure 9.

Figure 6.   Ten-inch Cleaning Plug in Header
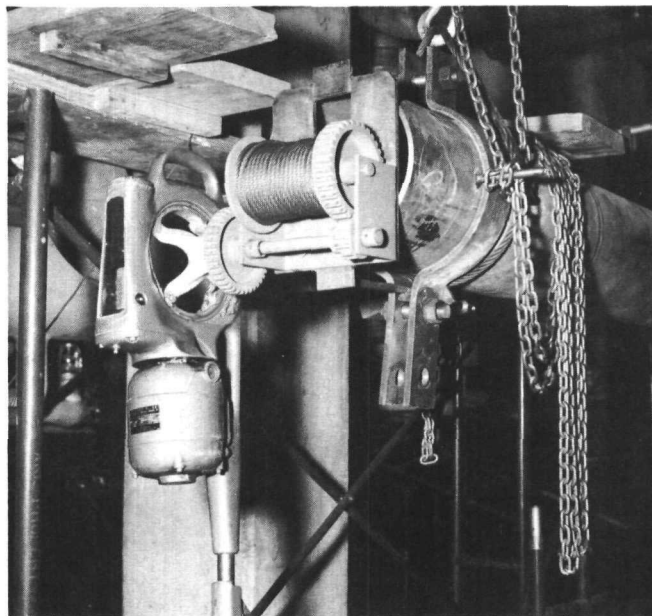
Figure 7.   Winch and Portable Power Drive for
Pulling "Pigs" through Pipe.
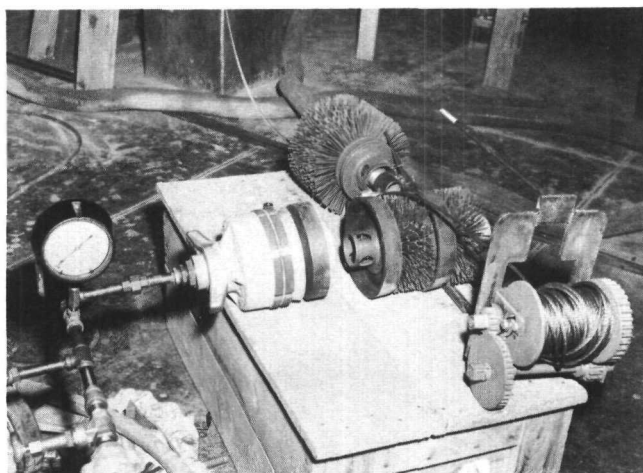
Figure 8.   Cleaning Pigs, Pipe Plug, Air Attachments and
Mechanical Winch.

Figure 9.   Modified "Pig" for Removing Loose
Material.

   b.   Leak Testing of the Evaporators - The Laboratory has completed
a helium leak test of the eight evaporators in the EBR-II Sodium-Boiler
Plant. This was a repeat of the test performed by the Construction Contrac-
tor at the time of receipt of the units from the Laboratory. These units now
have been tested three times to provide assurance of leak tightness at each
stage of "contractual responsibility," i.e., prior to shipment from the Labo-
ratory, upon receipt by the Contractor, and now upon return to the Laboratory
as a part of the construction responsibility assumed by the Laboratory as a
result of the Commission's default action against the Contractor.

All eight units successfully passed the first two tests; however, during the last test, one unit was found to leak. The leak exists in the vicinity of the lower sodium tube sheet; the exact location cannot be determined with the unit in place. The test indicated a leak of about 1.9×10^{-6} Std cc/sec in the lower sodium tube sheet of evaporator No. B3-EV-702. No leak was observed in any of the other units when checked with a helium mass spectrometer operating at a system sensitivity of about 5.7×10^{-10} Std cc/sec. Evaporator B3-EV-702 will be removed from the system, returned to the Laboratory, and repaired as quickly as possible.

As a further complication, the unit in question had been previously "abused" by the Construction Contractor during a cleaning operation. This occurred when the Contractor permitted blasting sand to enter the unit and subsequently removed the unit, tilted, vibrated, and vacuum cleaned it, etc., to remove the sand. In the process, he bumped the lower end, and also allowed the unit to stand on the lower end.

c. Modification of the Secondary Sodium Storage Tank Supports - The original design of the 16,000-gallon secondary sodium storage tank supports as provided by the Architect-Engineer are shown in Figure 10. They consisted of three supports each of which was welded to the tank in four locations. Longitudinal thermal expansion was provided by permitting the middle and foremost support to slide on permanently lubricated bearing plates. Flexibility of the support legs was to provide circumferential thermal expansion. Subsequent stress analysis of these support members indicated that the flexibility was inadequate. Redesign of the supports was necessary.

Figure 10

Original Supports for Sodium Storage Tank

The new supports have been installed and are shown in Figure 11. The modification consisted of first, removing the center support; second, cutting the center legs of each support free from the tank; and third, replacing the outer legs of each support by a pinned leg. The center support that was removed is shown in the center foreground of Figure 11. By cutting free the center legs of the remaining two supports and providing pinned outer legs, the tank can expand virtually unrestrained in a circumferential direction. The bearing area between tank and support was increased by providing a full cradle between the two center support legs. Stopper plates welded to the tank transmit the longitudinal movement of the tank to the support. The furthermost support remains anchored to the floor; the support in the foreground continues to provide longitudinal thermal expansion as originally provided.
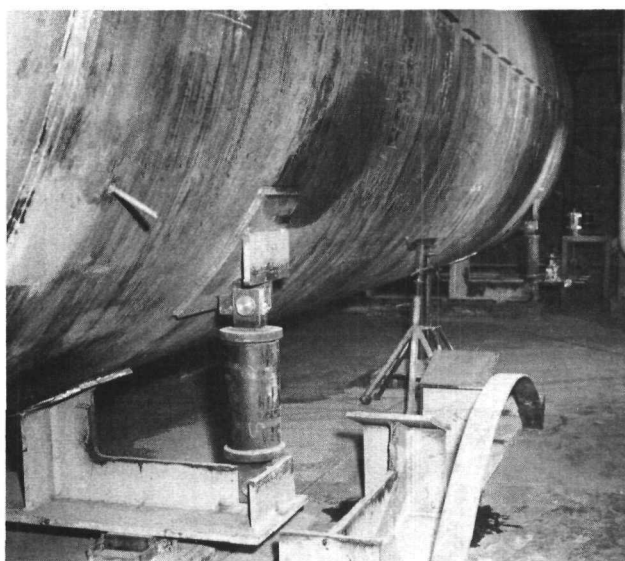
Figure 11

New Supports for Sodium Storage Tanks

d. Modification of the 10-inch, Non-Return Steam Valve - The original design of the steam system incorporated a 10-in. non-return valve in the superheated steam header from the steam generator. Subsequent analyses indicated that the non-return feature could be deleterious to system operation since at low steam flow rates the valve plug might tend to rise and fall. To prevent such an unstable behavior, the two-piece stem plug was replaced with a one-piece stem plug. The valve now acts as an ordinary shutoff valve.

2. Preparation for Dry Critical Experiments

Preparations for the dry critical experiments have continued and are essentially complete. As reported previously, this work consists primarily of minor corrective actions and modifications, checking out of the mechanical equipment and electrical circuitry, final alignments and adjustments of components and equipment, etc. The current status of this work is very briefly reviewed below.

a. <u>Control and Safety Rods</u> - All twelve control rods have been loaded into their respective thimbles in the reactor. Each rod has been tested individually with the reactor cover lowered into place. While any one rod is being tested the other eleven control rods are in the "down" position. Briefly, the checkout sequence for each rod consists of:

(1) Rod is raised to maximum "up" position.

(2) Rod is operated up and down as though regulating power level.

(3) Rod is raised to maximum "up" position.

(4) Rod is raised again to maximum "up" position.

(5) Rod is lowered to the "down" position.

Scram time-displacement characteristics have been measured for each rod and satisfactorily corroborate the curves obtained from tests made on the units prior to their installation in the reactor.

The two safety rods have been loaded into the reactor and the drive mechanism thoroughly tested for operation and scram.

b. <u>Nuclear Instrumentation</u> - The nuclear instrumentation for dry critical startup has now been checked out and is ready for operation. Isolation of equipment,cable shielding and grounding was required to eliminate "ground-loop" noise. The most troublesome difficulty, leading to a large number of spurious scram signals, has been with the temporarily-installed in-core detector channels. A defective amplifier has been replaced. Also, it has not been possible to shield these as well as the regular operating channels.

With all dry critical in-core instrumentation installed and the neutron sources installed, count rates have been determined for the in-core instruments as well as for the "J" thimble fission counters. The instrumentation channels are providing satisfactory response. The radiation level for personnel access into the primary tank with both sources in their respective shield thimbles was checked and the levels were found sufficiently low for personnel to work in the area. The maximum gamma level was 30 mr in one small spot, but the general level was less than 10 mr in the area over the sources.

c. <u>Fuel Handling Center</u> - The fuel handling control system was employed almost daily for subassembly transfers using procedures closely approximating actual dry critical operations. The handling operations included:

(1) Trial loading and transfer operations using a dummy source.

(2) Loading two active sources.

(3) Transfer of the sources to various core and blanket positions to facilitate testing and calibration of the nuclear instruments.

(4) Loading the control and safety rods.

The performance of the control system has in general been very satisfactory. The remaining unresolved difficulties consist mainly of transient disturbances in the information received from the position encoders. These appear to be caused by externally induced voltages in the long cables running to the encoders. Temporary circuit modifications have been made to compensate for the present difficulty with the gripper force-sensing devices.

3. Engineering

a. <u>Primary Tank</u> - The EBR-II primary tank and its "T-1" support structure are completely independent of each other on all sides except the top. The primary tank is supported at the top with six hangers which transfer the load of the tank and its contents to the "T-1" structure through six ultra-high strength rollers. This method of support allows the primary tank to undergo unrestricted thermal expansion, both radially and longitudinally. The detailed design of the hangers and rollers has been made to ensure that the radial thermal growth will occur symmetrically about the vertical centerline of the primary tank.

A series of measurements have been planned to verify this design feature. These tests are scheduled to occur after dry critical experiments and prior to loading sodium into the tank. The measurements will be made at several temperature levels of the primary tank, which will be heated with air to the highest temperature attainable (perhaps as high as 500°F). Measurement of the vertical displacement of the primary tank cover relative to the top structure at elevated temperatures will also be accomplished at this time. The vertical displacements will again be measured during and after filling the tank with sodium. The results of these latter measurements will provide data which will be used to verify the calculated effects of the sodium load on the deformation of components of the primary tank.

b. <u>Shield Design</u> - Calculations were made to estimate the heating at points in the EBR-II core and blanket regions caused by gamma rays from fission products, primary sodium, and steel activity. One hour after shutdown the heating due to fission product gamma-rays ranges from about 1.6×10^{-3} watts/cm^3 at the outside of the outer blanket to about 9.6 watts/cm^3 in the core. The heating from the primary sodium activity at the outside of the outer blanket is estimated to be 5% of the heating from fission product gamma rays. Steel activity heating in the outer blanket is much lower than the heating from sodium radiation.

4. <u>Procurement</u>

The sodium-to-sodium heat exchanger is now at the EBR-II site. Ten tank cars of sodium have been received at the NRTS site. The tank cars will be transported to the EBR-II site by motor truck in the near future.

5. <u>Component Development - Steam Generators</u>

The modification to the spare evaporator for use as a superheater is almost complete. The core tubes have been secured in place; the steam head has been rewelded in place, radiographed, and stress relieved, and the extension to the sodium nozzle has been installed.

The second modified evaporator has the flow baffles installed, the tubes in place, and both sodium tube sheets welded to the shell. Delivery of these two units should be made within the coming month.

6. <u>Component Development - Fuel Reprocessing Facilities.</u>

a. <u>Fuel Cycle Facility</u> - The Fuel Cycle Facility is more than 95 percent completed. Installation of services is continuing.

Work is being continued on the equipment that will be used within the Facility. A magnetic lifting tool for handling scrap containers within the Argon Cell has been received and is being adapted to manipulator operation. The control panels for the melt refining furnaces will soon be shipped to Idaho.

Mixtures of Shell APL and Standard Oil Company's NRRG-159 radiation-resistant greases are being irradiated and tested. Roller bearings are lubricated with the irradiated greases and then tested under an 800-lb axial load at 40 rpm. The first sample completed a successful test over the required cumulative running time of 76 hours, which is equivalent to about one year of operation in either cell of the Fuel Cycle Facility.

A calibration method has been devised which will permit the estimation of melt temperatures in the melt refining furnaces of the Argon Cell. The special calibration is made necessary because of the heat that will be generated within the furnace crucible by the irradiated pins. In the preliminary calibration test, the fission product heat source was simulated by placing resistance heaters within the crucible. The temperature of the reference thermocouple located at the bottom of the furnace susceptor was plotted as the ordinate, and the output of the motor generator power source was plotted as the abscissa. Temperatures within the crucible were measured by means of a thermocouple situated near the bottom

of the crucible. On the plot, the temperatures within the crucible appear as parametric curves. For practical application to the melt refining process, it is planned to establish a similar calibration grid by making a few accurate measurements of melt temperatures in the furnaces in the Argon Cell.

Three runs were made in which the melt from the melt refining of a uranium-fissium alloy was poured into a graphite mold and the resulting ingot was recycled for the next melt. The purpose of this procedure was to determine the amount of carbon picked up by the ingot from the graphite mold. Analytical results show that about 10 ppm carbon was introduced into the ingot in each pour.

b. Development of Remote Fabrication Equipment - The design and engineering of the EBR-II fuel refabrication equipment is estimated to be 91 percent complete. Work completed during the reporting period included the design, details and specifications for the bonding machine and for a part of the fuel element assembly and welding equipment.

The fuel pin processing equipment has been placed on bid with quotations to be received by August 31. Designs were completed and all materials were ordered for the electro-pneumatic control equipment to be placed in the sub-cell area. The fuel rod welding machine is about 95 percent complete. Detailed specifications must be written for this equipment.

The design of a prototype Fuel Subassembly Dismantler is nearing completion. The dismantler, together with Model 8 manipulators and other handling devices, will perform the operations required to remove the fuel and blanket elements from a fuel subassembly. About 75 percent of the parts for the dismantler are nearly ready for fabrication or are being fabricated. A device is being designed (with the aid of results from an experimental model) for removing the individual fuel elements from the support grid in a manner that will account for the position of each fuel element in the hex array.

Under normal conditions it is expected that the hex tubing forming the outer sheath of the fuel subassembly, after being cut free at the bottom end, can be pulled off from the core. In case this is not possible, several experimental devices have been built to slit the tube along its axis by using rolling cutters. The current design has made satisfactory cuts after 70 to 80 passes.

All of the devices required to inspect the fuel elements as they come from the dismantler and to load them into magazines have been fabricated and are being checked out. The fuel elements are inspected for excessive bow which would prevent their passing through the regular decanner. The magazine and carrier are used in transporting the fuel elements from the air into the Argon Cell where the decanning is carried out.

The principal unit of the Fuel Element Decanner, the spiral decanning unit, has been fabricated and a final inspection is being made before making operational tests. The remaining primary components of the decanner have been released for fabrication and are expected to be completed within two to three months. The balance of the decanning devices used for scrap disposal, chopped fuel transfer and fuel pin sampling, as well as devices to aid in manipulation are in the final stages of design.

7. Process Development

    a. Melt Refining Process Technology - Analytical results have been received on the third melt refining experiment (see Progress Report, March, 1961, ANL-6343) in which highly irradiated EBR-II prototype fuel pins were used. A 362-gram charge of ten percent enriched uranium-five percent fissium alloy, irradiated to 0.86 total atom percent burnup and cooled for 14 days, was melt refined for one hour at 1400°C. Despite the shorter time of melt refining (one hour compared to three hours in previous runs), the fission product removals were substantially the same as those obtained in runs which have been reported previously (see Progress Reports for November, 1960, ANL-6269, and July, 1961, ANL-6399). The fission product removals obtained in the present run were as follows:

Element	Percent Removed
Rare Earths and Yttrium	>99.0
Tellurium	98.9
Zirconium	20.5
Iodine	99.8

Complete material balances on fission products are not yet available since the melt refining crucibles and the volatilized fission products have not been analyzed.

    Construction of apparatus for the determination of nitridation rates of irradiated fuel pins in nitrogen-argon atmospheres has been completed. The apparatus will be tested with inactive material before the apparatus is installed in the Senior Cave.

    b. Skull Reclamation Process - Two experiments were performed to determine whether a chemical equilibrium could be demonstrated for the reaction

$$U_3O_8 \text{ (in flux phase)} + 8 \text{ Mg (in zinc phase)} \rightleftharpoons 3 \text{ U (in zinc phase)}$$
$$+ 8 \text{ MgO (in flux phase)}$$
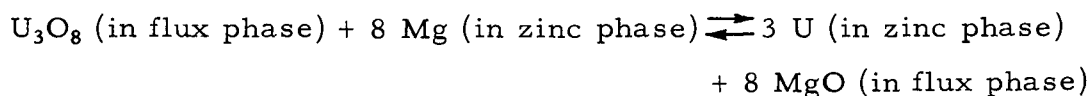
A calcium chloride-magnesium chloride-magnesium fluoride flux was used, and the equilibrium was approached from both directions. In the two experiments, the final uranium and magnesium concentrations in the metal phase after six hours were identical within analytical accuracy:

Final Concentrations in
Metal Phase

Mg (w/o)	U (w/o)
3.97	93.5
3.95	93.3

These results tend to support the hypothesis that the degree of reduction is limited by equilibrium effects rather than by rate effects. Additional work is needed, however, to verify this result.

The rate of reduction of zirconium oxide of the type used in melt refining crucibles by magnesium-zinc alloy proved to be lower at five weight percent magnesium than at 12 weight percent. The rate of reduction, however, is still sufficiently high with five percent magnesium-zinc alloy to introduce significant amounts of zirconium (under process conditions, about 0.1 percent) into the process stream. Further studies are being planned to determine the behavior of crucible zirconia during the reduction of uranium-fissium oxides.

The use of beryllia crucibles for retorting the uranium product continues to show promise. An isostatically pressed beryllia crucible (4-in. OD x 9-in. high) has now been employed in two runs and shows no signs of failure. The runs consisted of uranium dissolution, intermetallic compound precipitation and decomposition, and final retorting. About 99 percent of the uranium present at the retorting step was readily dumped from the crucible after retorting.

Preliminary indications suggest that the addition of U_3O_8 to a lithium chloride-magnesium chloride melt results in a mixture of uranium (IV) and uranyl ion in solution.

c. Blanket Processing - In the blanket process, the high solubility of plutonium and the low solubility of uranium in a magnesium-rich zinc solution is utilized to effect a separation of these elements. Analyses of separated magnesium-rich solutions (initial supernatant solution and a succeeding wash in which a 50 weight percent magnesium-zinc solution was used) indicate a slight physical carryover of uranium. Uranium concentrations in the separated phases were 0.11 percent in the supernatant solution and 0.05 percent in the wash solution as compared to a measured solubility of uranium of 0.025 percent at the separation temperature of 400°C. This is not regarded as being serious, but the carryover could probably be reduced, if necessary, by use of coarse filters in the transfer lines. A preliminary experiment indicated that uranium solubility in magnesium-rich zinc solutions may be lowered considerably by the addition of calcium (an 18 percent calcium concentration was employed in the study).

d. Plutonium Recovery Process - A consideration of the data on the extraction of cerium from plutonium by calcium and calcium-zinc solutions indicates that practical separation of the rare earths from plutonium in zinc-containing systems is feasible. It is estimated that, for a reasonable set of conditions in a conceptual process, about 95 percent removal of rare earths could be achieved, with a plutonium loss of about 0.5 percent. Further work is required to test the soundness of the concepts that are involved in the process scheme.

e. Materials and Equipment Evaluation - Two material demonstrations runs were conducted with flame-sprayed and sintered tungsten crucibles containing zinc-magnesium-uranium solutions and salt flux at 700°C for 7 hours and at 800° to 850°C for 68 hours, respectively. No corrosion was evident; however, the porosity of the crucibles permitted appreciable loss of zinc by diffusion of the vapor through the wall.

Tantalum filters have been obtained for mounting tantalum tubes used to sample liquid metals. Preliminary examinations and tests indicate that these filters, which are more inert to process solution constituents (particularly uranium) than are the presently used graphite filters, have the proper physical characteristics for this service.

8. Fuel Development - Core II.

a. Fast Reactor Fuel Jacket Development - The desired higher operating temperatures for liquid metal cooled fast flux reactors and the use of plutonium alloys or other fuels which are not compatible with stainless steel at desired reactor operating temperatures require the development of new high-strength alloys for jacketing material. Most development work to date has been limited to available vanadium, niobium and tantalum-base alloys.

Five more niobium-base alloys were cast, jacketed in 304 stainless steel, and hot rolled at 1150°C. The alloy strips are in the process of being removed from the cans prior to being cold rolled into sheet. The four niobium-base alloy strips mentioned in the July Progress Report (ANL-6399) have been cold rolled to 0.028-in. thick sheet.

Approximately 50 ft of Hastelloy-C tubing measuring 0.156-in. ID x 0.009-in. wall has been received and is in the process of being tested. The tubing has been radiographed and sectioned to remove defects (cracks, tears, etc.), as determined from evaluation of the radiographs. Following this the tubing was hydraulically pressure tested at 9000 psi, approximately 200 lb below the yield point of the tubing. The tubing is now being processed through the final test which consists of leak checking with a helium mass spectrometer.

III. REACTOR SAFETY (040117)

A. Thermal Reactor Safety Studies

1. Fuel-Coolant Chemical Reactions

Knowledge of the nature and extent of chemical reactions with nuclear reactor core metals that may occur in pressurized water or steam is essential to safe operation of reactors. The principal laboratory procedure uses a condenser discharge to provide almost instantaneous heating and melting of metal wire in water or steam. The energy input to the wire indicates reaction temperature; the transient pressure measures reaction rate; light emission indicates time-temperature; hydrogen generated gives extent of reaction; and particle size of the residue indicates the surface area exposed to reaction. A second method consists of heating the metal inductively and subjecting it to a steam pulse to induce a metal-steam reaction. A levitation method for studying metal-water reactions is being developed because the condenser discharge method fails when applied to aluminum. Steam is passed over levitated metal spheres in this procedure.

Studies of the kinetics of metal-water reactions under reactor incident conditions are being made in the TREAT reactor.

A series of condenser discharge runs with stainless steel wires in water was initiated. Preliminary results indicated that more extensive reaction occurred in heated water than in room temperature water. Results are, therefore, similar to those reported for zirconium and uranium.

Further studies of the uranium-steam reaction and the sodium-steam reaction indicated that results are similar, suggesting that rates are limited only by the diffusion and mixing processes within the reaction cell.

Four transients were completed in TREAT on fuel pins with a uranium dioxide core (20 percent enriched) clad in 18-mil thick stainless steel-304. The data obtained from these meltdowns in 25°C water are given in Table VI.

The data on the experiments with UO_2 core pins indicate a progressive increase in the amount of cladding (SS-304) -water reaction as the reactor burst becomes more energetic. For periods in the range 48 to 116 milliseconds, the extent of metal-water reaction from the correlation is 0.3, 5.5, and 19.0 percent stainless steel reacted for energies of 125, 225, and 325 megawatt-seconds, respectively. For these uranium dioxide core fuel pins, the dividing point between destructive and nondestructive transients (on fast periods of 48 to 116 ms) is a burst of about 130 mw-sec or 174 calories per gram of core. This corresponds to a peak central core temperature of 2200°C for adiabatic heating of the uranium dioxide.

Table VI. Results of TREAT Experiments on SS-Clad UO_2 Fuel Pins

	CEN Transient Number			
	64	65	67	66
Megawatt-second burst:	140	190	185	230
Millisecond period:	115	50	290	97
UO_2 core density, % of theor.:	89	89	98	98
% of SS-H_2O reaction:	0.8	5.2	0.3	9.0
Final appearance of fuel pin:				
Stainless Steel cladding:	two small ruptures, darkened area	fragmented, part melted	intact, darkened central area	fragmented, part melted
UO_2 core:	distorted, cracked	fragmented, fine particles	radial cracks	fragmented, coarse particles

2. Kinetics of Oxidation and Ignition of Reactor Materials

Studies are being made of the oxidation and ignition kinetics of the metals uranium, zirconium, and plutonium in order to provide information leading to an understanding of the reactions. This knowledge should make it possible to minimize the hazards associated with handling these nuclear reactor materials. Isothermal oxidation on microscope stage, shielded ignition, burning curves, rate of propagation of burning foil, and burning temperatures are the techniques being used. In the continuing study of ignition and burning of uranium, zirconium, and plutonium, more emphasis is being placed on the burning process. Burning propagation rate studies provide a useful tool to observe the effects of many variables. The effect of the presence of halogenated hydrocarbons on the burning of uranium foil in air is being investigated.

Studies of the isothermal oxidation rates of uranium in the "heat sink" apparatus in the 300° - 500°C range are continuing. Rates increased 20-fold with an increase in temperature from 300° to 400°C with Argonne base uranium. Rates were nearly constant in the range from 400° to 500°C.

Ignition studies of zirconium foil were completed. The studies were made under conditions where no pre-oxidation film would be present before suddenly bringing the specimen into contact with oxygen at the test temperature. The foils were suspended on platinum supports and sealed into quartz vials under high vacuum. The oxidation film present at room temperature and residual air were dissolved into the zirconium by induction heating the metal within the vial to 1400°C for several minutes. Vials were then brought to the test temperature in a steel bomb containing pure oxygen. Vials were broken and it was determined visually whether ignition occurred or not. Results showed general agreement with data obtained by the shielded ignition method. Calculations quantitatively relating ignition results to isothermal data are underway.

B. Fast Reactor Safety Studies

1. Core Meltdown Studies - TREAT Program

TREAT in-pile experiments are being performed on fast reactor fuel samples in order to obtain information on the types of sample fuel movement and failure, and to survey the mechanisms producing such phenomena.

a. Oxide Sample Experiments - The remaining two samples (Nos. 4 and 5) from the first meltdown experiment series on oxide fuel (ANL-6399, July Progress Report, pp. 38-39) were given a macroscopic examination. Both samples 4 and 5, for which maximum cladding temperatures of 1375°C and 1500°C, respectively, were measured, were found to have cladding failure and regions in which the steel EBR-II cladding had melted. In neither case was there fuel fragmentation although the intact fuel pellets contained fissures and central cylindrical regions of marked difference in appearance. Pieces from samples 4 and 5 were taken for metallographic examination. Pieces from samples 2 and 3 (maximum measured cladding temperatures of 900°C and 1200°C, respectively) were studied under a microscope. Both showed the same structure as an unexposed control specimen.

Preparations have begun on capsules for the second series of meltdown experiments on oxide fuel, Series XXV. Two samples are clad with stainless steel EBR-II jackets and will be used to study possible changes in effective fuel-cladding interface thermal conductance and fuel sample structure brought about by successive transients below that necessary to produce cladding failure. The remaining two samples of S-XXV will be clad with tantalum tubing the size of EBR-II jackets and will be used for single input transients of higher energy.

b. EBR-II Elements in Stagnant Sodium - The remaining three capsules of the second series (XIX) of meltdown experiments on EBR-II elements in stagnant sodium were opened and examined, as were the three stagnant sodium capsules of S-XXIII run during the previous report period. A brief summary of the S-XIX and S-XXIII results is given in Table VII.

The last two capsules of XXIII were run at TREAT. The capsule with the pressure transducer damaged in transit was given a sample energy input about 10% greater than the largest previous stagnant sodium input. The fifth capsule of the series contained an EBR-II Mark-I element of natural enrichment (instead of the 3% enrichment used for all other stagnant sodium experiments to date), internally instrumented with a miniature tantalum-clad, tantalum-molybdenum thermocouple. Both capsules are being returned for examination.

Table VII. Results of TREAT Meltdown Experiments on EBR-II
Elements in Stagnant Sodium

Experiment		Nominal Reactor Energy Release, Mw-sec	Sodium Bath Pressurized to Prevent "Slugging" of Coolant	Condition
XIX	1	180	No	No cladding failure, small voids in fuel. Small fuel-clad alloying.
	2	170	No	Same as above.
	3	161	No	No cladding failure, no fuel voids, small amount of alloying.
	4	180	No	No cladding failure, fuel voids (one almost the size of fuel diameter). Extensive alloying.
XXIII	1	144	No	Same as XIX-1.
	3	146	Yes	Same as above.
	4	180	Yes	Extensive failure at bottom; top of cladding unfailed with extensive alloying inside.

c. **Photography of Dry Meltdown Specimens** - All five tests of the second series of photographed meltdown experiments (XXIV) were performed. The new, white background arrangement produced good delineation of samples and material movement occurring after sample failure. Two Fermi-I elements were run, one to mild failure and the other to extensive failure. Molten uranium streams from the samples showed up clearly, permitting estimates to be made of droplet or stream size, trajectories (as an indication of internal sample pressures), and timing of failures. Formation of voids inside the cladding as the uranium fuel ran out could be detected by noting variation in color along the length of the samples.

Two stainless steel clad EBR-II, Mark-I samples were exposed. One was carried to the approximate threshold of extensive failure, and the other, appreciably beyond the threshold. Both showed the characteristic sharp circumferential expulsion of bond sodium. Initial velocities of the fronts of the sodium clouds were consistent with estimates of internal sample pressures due to heating of sodium and the inert gas inside the sodium expansion volume at the top end of the element. Attempts were made to estimate the duration of bond sodium expulsion quantitatively by timing the duration of appreciable cloud turbulence.

In addition, the high temperature failure of a tantalum-clad EBR-II pin due to internal pressure was also observed. A succession of cladding failures each accompanied with release of sodium was seen,

consistent with a "progressive splitting" failure. For this last test, a speed of about 4000 frames/sec was employed, and sodium cloud turbulence again was easily observable. All five capsules from this series have now been received for examination.

2. Calculations of Transient Fuel Element Temperatures

An IBM-704 heat transfer program RE-248 ("Argus"), has been developed to calculate temperatures in a cylindrical geometry as a function of time, radius, and axial position. This program is an outgrowth of an earlier transient heat transfer code, RE-147 ("Cyclops") (ANL-6295, December, 1960 Progress Report, p. 39) which has been used extensively for calculation of TREAT sample temperatures. Special features of Argus include the following:

(1) Provision for up to twenty-five concentric regions.

(2) Any region may be either "solid," with space- and time-dependent heat generation, or "coolant," either static or flowing.

(3) Solid material properties are approximated as constants over input temperature ranges. A maximum of ten temperature ranges may be used. There are provisions for phase changes.

(4) Coolant properties are approximated by second-order polynomials in temperature.

(5) Heat transfer by conduction, convection, and radiation is considered, and provisions are made for surface and bulk boiling of coolants.

(6) Surface conductance between adjacent regions is included.

(7) "Thin" regions (for example, the sodium bond of EBR-II elements or the zirconium cladding of Fermi-I pins) can be put in explicitly, rather than lumping them with adjacent material.

(8) Coolant flow is specified as a function of time.

3. TREAT - Component Development

a. Fission Rate Distribution in TREAT Core - Because the stainless steel transparent capsule assemblies caused considerable warping of the flux in the core, which in turn changed the control rod and nuclear instrument calibrations, the fission rate distribution in only the east half of the core was mapped in detail. It was found that a flux peak occurred in the north half of the reactor approximately 12 in. from the core center. This peak had an amplitude 1.4 times the central fission rate value, and the

central to core average fission ratio was found to be 1.02. The flux at the transient operating instruments on the north side of the reactor increased by 25%, while on the south side, it decreased by approximately 2%.

    b.   <u>Transparent Facility</u> - Two calibrating transparent capsules have been assembled and fired in TREAT. These were 6% enrichment EBR-II fuel elements which had small uranium disc foils mounted at various points on the cladding of the fuel elements. After disassembly, the uranium foils were analyzed chemically for particular fission products. These data are used to correlate reactor power levels (as determined from the nuclear instruments) with the power developed in the samples.

    c.   <u>Small Sodium Loop</u> - Four small bayonet-type sodium loops are being constructed for flowing sodium experiments in TREAT. A loop will fit into the reactor as an integral part of a special TREAT element. The first loop is complete.

The fuel element remover was fabricated and assembled. Following preliminary testing the first sodium loop was satisfactorily disassembled using this tool. The sodium was removed from the first loop and then all components were thoroughly cleaned, reassembled, and readied for a new clean sodium charge. A sodium purifier has been fabricated, welded, and assembled. Nine charges of sodium can be obtained from this purifier.

4. TREAT Construction

The construction contractor completed the additions to the Control and Reactor Buildings and the buildings were accepted by the Commission on August 15, 1961.

IV. NUCLEAR TECHNOLOGY AND GENERAL SUPPORT

A. Applied Nuclear and Reactor Physics

1. 3.0 Mev Van de Graaff

a. **Determination of $\bar{\nu}$ and $d\bar{\nu}/dE$** - The measurements of $\bar{\nu}$ and $d\bar{\nu}/dE$ for U^{235} have been extended. Final analysis of the U^{235} data gives

$$\bar{\nu}(U^{235}) = 2.43 + 0.098\ E(Mev)$$

and

$$\frac{d\bar{\nu}}{dE}(U^{235}) = 0.098 \pm 0.007\ Mev^{-1}$$

[The Progress Report for July, ANL-6399, contained a misprint: $\frac{d\bar{\nu}}{dE}(U^{235}) = 0.10 \pm 0.07$ should have read $\frac{d\bar{\nu}}{dE}(U^{235}) = 0.10 \pm 0.007$, as indicated in Figure 9, page 41 of ANL-6399.]

Measurements of $\bar{\nu}$ have also been made for Th^{232} and U^{238} at an incident neutron energy of 1.60 Mev, and for Cf^{252} spontaneous fission. All measurements were made relative to the "total" (prompt + delayed neutron) $\bar{\nu}$ for thermal fission of U^{235}. The results are:

Nuclide	Energy (Mev)	$\bar{\nu}$(prompt + delayed)
Th^{232}	1.60	2.195 ± 0.042
U^{238}	1.60	2.594 ± 0.036
Cf^{252}	Spontaneous	3.757 ± 0.046

b. **Delayed Neutron Measurements** - Measurements of the delayed neutron emission as a function of incident neutron energy have been made for the fast neutron induced fission of Th^{232}, U^{238}, and U^{235}. Both the time dependence of the delayed neutron activity and the total yield were measured. The U^{235} data were taken at five neutron energies between 250 kev and 1500 kev. Measurements were made at 1500 kev and 1650 kev for Th^{232}, and at 1400 kev, 1500 kev, 1600 kev, and 1750 kev for U^{238}. No change was observed in the time dependence behavior for any of the nuclides. The total delayed neutron yield was constant within the experimental uncertainty of ±5% for U^{235} and Th^{232}. For U^{238} the total delayed neutron yield increased 28% ± 5% between incident neutron energies of 1400 kev and 1750 kev. The change observed in the delayed neutron yield for U^{238} is probably due to penetration of the fission barrier. Further investigation of the sub-threshold fission of U^{238} and Th^{232} is planned in an effort to determine the effect of barrier penetration on the delayed neutron yield.

c. <u>Fast Neutron Capture Cross Sections</u> - The neutron activation cross section measurements of I^{127} and In^{115} (n,γ) In^{116} (13 sec) have been completed. The absolute normalization of the I^{127} cross section is based on the U^{235} fission cross section and the Au^{197} activation cross section of 0.137 barns at E_n = 600 kev. The absolute normalization of the In^{115} cross section is based on the In^{115} (n,γ) In^{116} (54 min) activation cross section of 0.160 barns at E_n = 600 kev and the thermal neutron activation cross sections for the 13-second and 54-minute activities from In^{116}. The estimated uncertainty for the iodine cross section is $\pm 15\%$, and for the indium cross section $\pm 20\%$. The results are given in the Table VIII.

Table VIII. Neutron Activation Cross Sections of I^{127} and In^{115} (13 sec)

E_n (kev)	σ (Iodine) (barns)	σ (Indium) (barns)	E_n (kev)	σ (Iodine) (barns)	σ (Indium) (barns)
175	-	.163	950	.073	-
200	.250	.192	1000	.069	.205
280	.200	.185	1050	.062	-
300	.164	.175	1100	.063	-
350	.147	.170	1150	.065	-
400	.133	.165	1200	.064	.205
450	.122	-	1250	.062	-
500	.107	.155	1300	.061	-
550	.101	-	1350	.060	-
600	.100	.160	1400	.056	.195
650	.093	-	1450	.054	-
700	.097	.170	1500	.055	-
750	.086	-	1550	.053	-
800	.079	.178	1600	.050	-
850	.074	-	1650	.051	-
900	.069	.195	1700	.050	-

2. <u>Argonne Thermal Source Reactor (ATSR)</u>

a. <u>Resonance Integral Measurements</u> - Several significant steps have been made in adopting the ATSR and its autorod control system to the measurement of resonance integrals. The reactor has been stabilized and preliminary measurements indicate that the sensitivity of the system will be very good.

Temperature measurements in the dump, shield, and core tanks of the ATSR, along with observations of reactor drifts, have indicated that the reactor becomes stable when the shield and core tank temperatures are approximately equal. By heating the water in the dump tank it has been possible to reduce the time required for the reactor to stabilize from five or six hours to less than an hour.

With the reactor thus stabilized it has been possible to accumulate sufficient data to make rough measurements of the resonance integrals of boron and Sm_2O_3 relative to a single gold foil standard. The measurements of boron have been made with an aluminum-boron powder mixture. Milligram quantities of boron were mixed with approximately 20 gm of aluminum powder. The preliminary data indicate that this method of dilution for boron will probably be effective. About 5 mg of boron give a reactivity change which corresponds to a 5% full-scale deflection of the autorod.

The autorod system has continued to work satisfactorily. The linearity of the rod has been checked and the rod worth has been found to be uniform within ±0.5% over its active length. Gold foil samples of different thicknesses are now being prepared. The extrapolated zero-thickness gold calibration will be made from the oscillation data obtained with these foils.

In order to study the effect of sample position on reactivity change caused by the insertion of a sample into the cadmium tube, a control rod drive has been temporarily mounted on top of the reactor. A sample can has been attached to the end of the drive unit with a nylon string in such a way that the sample rests on the bottom of the sample tube when the rod drive is in its down limit position. In its top limit position the sample is located about 4 in above the top of the core. Using the selsyn indicator in the control room it is possible to position the sample at any height in the core during a reactor run and then to observe the autorod position.

The 21-mg gold foil in a thin aluminum sample can, which has been used previously in the determination of autorod sensitivity, was observed to give a positive reactivity effect as it first enters the active zone of the reactor core. This positive effect increases to a peak which occurs about 2 in. into the core. As the sample is inserted still further into the core the effect is still positive but it becomes smaller until at a point 6 in. from the edge of the core its net effect is zero. Beyond this position the reactivity effect is a negative one which increases in magnitude until it reaches a rather broad maximum of about 10^{-6} $\Delta k/k$, which is found at the center of the core. As the sample is inserted still further into the core the negative effect decreases, the reactivity change passes through zero, reaches a positive maximum and again becomes zero as the sample reaches the bottom of the active zone of the core.

3. ZPR-VII - High Conversion Critical Experiment

Experimental work has proceeded on the 621-element (BORAX-V 4.95 wt-% enrichment) core. This is a square lattice (1.27 cm spacing) loading which gives a ratio $H:U^{238}$ of 4.654. The reactivity worth of each of the five-fingered control elements is 1.52% $\Delta k/k$. There are four of these elements. There are also four blade rods at the periphery of the core which are worth about 0.22% $\Delta k/k$ each. The worth of the top reflector

has been determined as 0.33% $\Delta k/k$. The radial and axial reflector savings have been determined from fitting flux traverses using IBM Cofit and Jofit codes. The radial savings are 7.2 cm. The top axial savings are 5.3 cm and the bottom axial 6.1 cm. This difference can be attributed to the presence of more stainless steel in the top reflector.

Measurements with gold foils indicate a flux of $4.75 \times 10^8 \, n/(cm^2)(sec)$ at the center of the core when the fission rate (determined radiochemically) is 1.98×10^{10} fissions/gm of fuel (also at the center). This corresponds to a power level of about 40 watts with a 621-pin core loading.

The fast effect has been calculated from activation of fission foils to be 1.038. This is to be compared with the value 1.054 computed using modified two-group theory. Data for the initial conversion ratio, resonance escape probability and thermal utilization are being processed.

A portable graphite thermal column has been constructed for use at the leakage face of ATSR. The gold-cadmium ratio at the center is about 94. This is sufficient for standard foil irradiation for the initial conversion measurements planned for the Hi-C program.

4. Experimental Nuclear Instrumentation

   a. Analog-to-Digital Techniques for Auto- and Cross-Correlation of Reactor Dynamics Data - Three REDCOR amplifiers and the buffer memory have been sent back to the manufacturer for repairs.

   b. Reactivity Measurement in Subcritical Cores - Work is continuing on methods of determining subcritical reactivity margin in existing or new reactors. A number of experimental techniques have been analyzed to see if they can be applied to this problem.

   c. Fast Neutron Spectrum Measurement - Proportional Recoil Counters - A study is in its beginning stages to determine whether long-range electrons due to gamma rays can be distinguished from short-range recoil protons through the differences of the rise times of the pulses. A special counter body adapted to this type of investigation has been constructed. A Cm^{244} source sends alpha particles parallel to the counter wire; it provides a calibration line which is not subject to saturation or shielding effects originating in high charge densities from ionization columns perpendicular to the center wire. The necessary circuitry is now being built.

   In parallel with this development, the performance of a propane-filled, 5-cm diameter recoil counter is being examined in order that its promises and limitations as a spectrometer in a fast assembly may be assessed. The following tests have been made:

Multiplication and resolution as functions of position in the counter have been examined by magnetically moving a small, collimated alpha-particle source from point to point and registering the counter output in the multichannel analyzer. It appears that the center wire in the counter is of uniform diameter, that end effects are confined to a region of about 2 cm in length at each end, and that multiplications beyond 50 produce resolutions beyond about 15%.

Response to 1 Mev neutrons from the Van de Graaff machine has been registered in a 256-channel analyzer. The applied voltage and the electronic amplification were varied from run to run. Resolutions of approximately 12% have been seen in the one run where statistics are good enough to permit the differentiation of the experimental curve. A noise component corresponding to somewhat less than 500 kev of ionization energy is visible in all curves. Its origin will need to be traced in a more elaborate investigation in the future.

d. **Fast Neutron Spectrum Measurements - Solid Counters -** A program of investigation of solid counters as neutron spectrometers has been initiated. A first test of the output from boron-diffused counters in a monoenergetic neutron beam has been made. The distribution of the pulses has been very flat, suggesting that the boron-containing region must be made extremely thin if good resolution is to be achieved.

5. Theoretical Reactor Physics

a. **Multigroup Calculations of Effective Delayed Neutron Fraction β_{eff}, Prompt Neutron Lifetime ℓ_p and Related Kinetics Parameters for Large Fast Plutonium Fueled Reactors** - For the plutonium-fueled fast reactor cores reported in ANL-6212[*] several parameters related to kinetics problems have been evaluated. For the 1500-liter cores the effect on these parameters of the following different isotopic concentrations of plutonium is being investigated:

(1) Pure Pu^{239};

(2) 74.7% Pu^{239}, 10.2% Pu^{240}, 12.4% Pu^{241}, 2.7% Pu^{242}

(3) 40% Pu^{239}, 10% Pu^{240}, 25% Pu^{241}, 25% Pu^{242}.

These systems used sodium coolant and stainless steel (or other high-temperature alloys) for cladding. Metal fuels are studied as well as PuO_2 and PuC mixed with either U^{238}, UO_2, and UC diluent respectively. The effect of core size was studied by analyzing Pu^{239} cores of 800, 1500, and 2500-liter for metal, oxide, and carbide fuels.

---

[*]S. Yiftah and D. Okrent, "Some Physics Calculations on the Performance of Large Fast Breeder Power Reactors," ANL-6212 (December, 1960).

The prompt neutron lifetime ℓ_p and the effective delayed neutron fraction β_{eff} have been evaluated by using a machine program which utilized as input the space and energy dependent flux and adjoint spherical geometry solutions for the reflected assemblies. This machine program can accommodate five fissionable materials. The formulas used to attain β_{eff} and ℓ_p follow essentially the definition given in a paper by D. Meneghetti.[*]

In order to be able to reason physically on the obtained parametric values the total number of fissions for each plutonium isotope as well as for U^{238} has been evaluated for all cores. Expressions proportional to the worth of prompt and delayed neutrons were obtained. All worth functions are related to the worth of a prompt Pu^{239} neutron in the core. Finally, β_{eff} values are obtained for each delayed neutron group. By using BUM, the Transfer-Function Code, the zero power transfer function, $ZP(jw)$, is obtained. The decay constants, λ, used in all cores are the ones for Pu^{239}.

b. <u>Burnup Characteristics of Plutonium-Fueled Reactors</u> - A study is being made of the burnup characteristics of plutonium-fueled, near-thermal reactors with the plutonium having an isotopic composition of 78 atoms of Pu^{239} to 12 atoms of Pu^{240} to 10 atoms of Pu^{241}. Long lifetimes are possible with such reactors because the Pu^{240} can serve as a combination fertile material and burnable poison. The burnup characteristics of such reactors are very dependent on spectrum since the Pu^{240} has a very large resonance at 1.035 ev and Pu^{239} has a resonance around 0.3 ev. In order to have the best burnup characteristics, the loading of the reactor should be such that the ratio of effective absorption cross section of Pu^{240} to that of the capture (absorption-fission) cross section of Pu^{239} is as large as possible. If the loading of plutonium is too light, the spectrum will be too thermal and the above-mentioned ratio will not benefit enough from the large resonance absorption of Pu^{240}. If the loading is too heavy, the spectrum will be highly epithermal, but the self-shielding of the Pu^{240} resonance will be too great to enable the resonance to be sufficiently effective.

Calculations of burnup are being made for two cases with the volume fractions of fuel, H_2O and steel similar to those in SM-1 lattices although the reactors in those calculations are being considered as homogeneous. MUFT and SOFOCATE cross sections are being used in the burnup calculations with the cross sections being redetermined several times during the burnup because of the sensitivity of effective cross sections to spectrum changes.

---

[*] D. Meneghetti, "Recent Advances and Problems in Theoretical Analysis of ZPR-III Fast Critical Assemblies." Submitted to IAEA Seminar on the Physics of Fast and Intermediate Reactors, Vienna, August 1961.

c.   <u>Study of Shape Factors in Fast Reactors</u> - The shape factor is generally defined to be the ratio of the critical mass of a system in spherical geometry to the critical mass of the identical system in cylindrical or slab geometry. Previous investigations (see Progress Report for November, 1960, ANL-6269) have now been extended to four fast reactor systems of varying L/D ratios. These have been analyzed to predict:

(1)   The variation of critical mass with core geometry.

(2)   The reactivity worth of fuel at the core boundary as a function of core geometry.

(3)   The power distribution as a function of core geometry.

The absolute values of these parameters are dependent on both the core and reflector compositions. Two of the systems represent a typical, low density, fast reactor and a typical, high density, critical experiment. The other two systems represent compositional combinations of the first two systems.

It was found that the optimum geometry, ratio of core height to diameter $\approx$ 0.9 shape factor tends to increase with core density. Therefore the optimum shape factor for ZPR-III Assemblies 22, 24 and 25 is about 0.99. A shape factor of about 0.93 is applicable to ZPR-III Assemblies 20, 23, 29, 30, 31 and 33.

The reactivity worth of fuel at the core boundary tends to increase with ln L/D, the ratio of core height to diameter. The ratio of maximum power density tends to be inversely proportional to ln L/D.

d.   <u>CP-5 Converter-Tube Analysis</u> - A decision has been made to install a converter-tube facility in the graphite reflector at CP-5 (see Progress Reports ANL-6343 and 6399). The converter will provide a total fast neutron flux ($E > 9.12$ kev) of 10^{12} n/(cm^2)(sec) and a thermal flux of less than 10^8 n/(cm^2)(sec) on the tube centerline. This facility will be used to study radiation damage mechanisms at low temperatures.

A hazards analysis is in progress to determine:

(1)   The multiplication factor of the converter tube for different environmental conditions, and

(2)   The effect of the loss of coolant water.

B. Reactor Fuels and Materials Development

1. Corrosion Studies

a. <u>Zirconium Alloys for Superheated Steam</u> - The alloys containing copper, nickel, and iron (see Progress Report, July, 1961, ANL-6399) have now been exposed for 50-60 days in steam at 540°C and 600 psi. In most cases it appears that corrosion behavior is undergoing transition to constant rate. These alloys are also being tested at 650°C and 600 psi and have been exposed for 35 days. All but the Zr-2 w/o Fe binary show a <u>decreasing</u> slope on the log-log plot (wt gain vs time) but it may be that this is due to spalling of oxide. This condition emphasizes the need for a different method of measuring corrosion rate.

The alloys containing titanium are being continued in test at 540°C and 600 psi. Variations of the original compositions have been prepared and samples are being prepared for hydrogen analysis. However, only the Zr-0.02 w/o Ti-0.21 w/o Pt alloy has satisfactorily survived 5.5 days in steam at 650°C and 600 psi.

2. Improved Fabrication Procedure for Zirconium Alloy Tubing

Small diameter zirconium alloy tubing which is free from internal defects has not been commercially produced. This type of tubing is in demand for instrumentation applications in light or heavy water-cooled or moderated thermal reactors. There is also a need for larger diameter thin wall zirconium alloy tubing for these reactors which is also not yet available commercially.

Six Zircaloy-2 hollow billets were successfully extruded into tubing. Three of the billets were machined from powder metallurgy product ingots prepared by the General Electric Company and the remaining three billets were machined from a 7 in. x 7 in. forged bloom of Mallory-Sharon vacuum arc melted ingot stock. The billets were machined to 0.934 in. O.D., jacketed in copper, and extruded at 725°C. The extrusion ratio was 8:1 and the extruded Zircaloy-2 tube measured 0.407 in. O.D. x 0.273 in. I.D.

Using the method of drawing with a core described in the July, 1961 Progress Report, tubes 0.080 in. O.D. x 0.050 in. I.D. were successfully produced from both the General Electric sintered Zircaloy-2 powder and the Mallory-Sharon vacuum arc melted ingot material.

The present procedure uses 0.407 in. O.D. x 0.273 in. I.D. extrusions, (net dimensions, without sheath), and a 0.252 in. cold drawn copper core. The sheath is pickled off the inside wall of the extrusion which is subsequently drawn with the copper core in approximately 20% drafts to the final dimension. Annealing at 500-600°C for 15-25 min is performed after every

60-70% cumulative reduction. These relatively mild annealing conditions, coupled with the protection afforded by the outer jacket and core, allow heating to be performed in an air furnace. After the third (final) anneal, the core is removed and the exterior bright pickled.

Microscopic examination and eddy current tests indicate freedom from internal cracking and a satisfactory internal surface. However, the outside surface is not quite satisfactory in view of the deep striations induced during extrusion which remain throughout all subsequent processing, including pickling. The outside surface can be conditioned, as is currently done in commercial practice, although one objective of this program is to eliminate this defect from the extrusion process.

3. Irradiation Studies

    a. Irradiation of ThO_2-UO_2 Fuel - Nine NaK capsules, each containing a single unclad pellet of 89.0 w/o ThO_2-10 w/o UO_2 (93.2% enriched) - 1.0 w/o CaF_2, have been punctured for measurement of released fission gas. These capsules have been under irradiation in MTR and have achieved burnups ranging from 17,600 to 22,900 MWD/T oxide at $\int kd\theta$ ratings between 31 and 50 w/cm. Eight of the pellets were cradled in stainless steel wool while the ninth was loosely held in a Zircaloy frame.

The irradiations were intended to evaluate the role of open pores in the release of fission gas. The pellets covered the range of open porosity from 0.17 to 15.70% with a total porosity range of 6.94 to 22.08%. Table IX contains a summary of the data.

Table IX. Effect of Irradiation on ThO_2-UO_2 Pellets

Spec No.	Open Porosity, %	Closed Porosity, %	Burnup, MWD/T	$\int_{T_s}^{T_0} kd\theta$, w/cm	Gas Release, % Theoretical	No. of Fragments
ANL-35-80	0.17	6.77	21,600	50	0.72	16
ANL-35-82	0.25	10.26	17,600	33	1.14	19
ANL-35-87	0.79	11.48	19,600	44	0.85	12
ANL-35-96	4.86	14.61	22,900	50	3.67	8
ANL-35-99	6.38	15.70	17,600	37	3.41	6
ANL-35-101	8.65	10.53	18,900	41	4.60	5
ANL-35-104	13.90	7.12	15,500	31	4.54	1
ANL-35-105	14.80	6.70	20,300	41	1.53	3
ANL-35-106	15.70	5.87	22,200	44	3.81	2

Eight of the pellets fractured and only one remained whole. The size of the fractured pieces increased and the number of pieces decreased with increasing open porosity. Low porosity pellets broke into an average of 16 pieces, while the medium porosity pellets average 6 pieces.

Two pellets that remained virtually intact, (ANL-35-104 and ANL-35-106) had high percentages of open porosity. The third specimen (ANL-35-105) with a high percentage of open porosity, was irradiated in the Zircaloy frame and its breakup into three pieces is partly attributed to mechanical shock.

The true effect of open porosity on fission gas release is probably masked by differences in irradiation temperatures. The breakup of the pellets lowered the irradiation temperatures because of the larger surface area exposed to the NaK coolant. The results seem to substantiate the expected relationship between porosity and gas release but the results can also be explained by the relative irradiation temperatures.

The three most porous pellets remained relatively intact so that their temperatures were higher, thereby promoting the release of more gas than the broken low porosity pellets. In this case, temperature was probably a more important factor than surface area in the release of the gas. Further irradiations are planned for clad specimens which will promote maintenance of the starting geometry.

b. <u>Irradiation of Refractory Alloy Clad Plutonium Alloys</u> - Three instrumented capsules, each containing six U-20 w/o Pu-10 w/o Fs fuel pins with various cladding materials, were irradiated in CP-5. NaK was used as a heat transfer medium in two capsules and sodium was used in the third. These were elevated temperature tests in which the intended control temperature was 650°C. Heaters inside the capsules were provided for temperature control when the reactor was at power. During irradiation, however, the specimen temperatures were much higher than desired because of unexpectedly high fission rates in the specimens. The capsules were positioned in the CP-5 fuel thimbles where a relatively hard neutron spectrum exists. Under these conditions the anticipated amount of flux depression in the plutonium alloy specimens did not occur.

In some cases temperatures as high as 1000°C were recorded. Since this is well above the 820°C melting point of the fuel it was expected that the specimens would show damage from overheating. Accordingly, the capsules were removed from the reactor for hot laboratory examination of the specimens after they had achieved burnups ranging up to 1.5 a/o.

Gamma autoradiographs of the contents of the capsules are shown in Figs. 12, 13, and 14. Unfortunately, no identification of individual specimens in the radiographs is possible, and more specific information must await opening of the capsules.

Many of the specimens are severely damaged; however, the bottom specimens in the capsule with sodium as a heat transfer medium seem to be in good condition, but they have been displaced with relation to each other in the capsule. Considering the manner in which the specimens were positioned in the capsule, high stresses must have been present to cause such displacements.
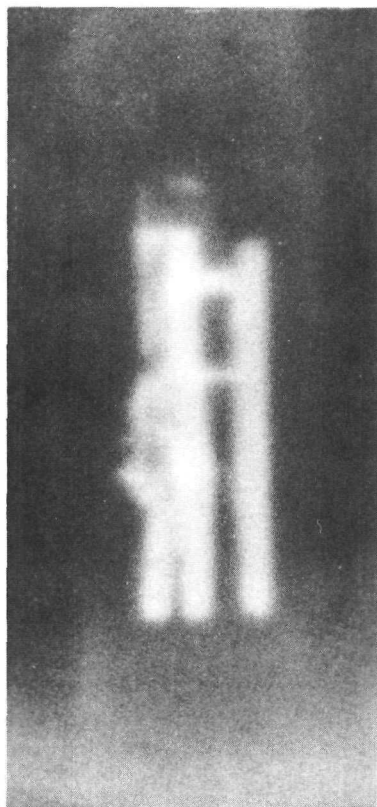
Fuel: U-20% Pu-10% Fs

Heat Transfer Medium: NaK

Reactor Power Output: 9,357,165 kwh

Top Section:

    Specimen Cladding (Individually unidentified)

    1. Inconel-X[a]
    2. Nb-1% Zr
    3. Vanadium

Figure 12

Autoradiograph of Capsule CP-16

Bottom Section:

    Specimen Cladding (Individually unidentified)

    4. Niobium
    5. Nb-1% Zr
    6. SS 304[a]

(a) Contained a $\frac{1}{2}$ mil thick vanadium barrier foil.

44

Fuel: U-20% Pu-10% Fs

Heat Transfer Medium: NaK

Reactor Power Output: 7, 788, 899 kwh

Top Section:

    Specimen Cladding (Individually unidentified)

      1. Nb-1% Zr
      2. Niobium
      3. Vanadium

Figure 13

Autoradiograph of Capsule CP-17.

Bottom Section:

    Specimen Cladding (Individually unidentified)

      4. Nb-1% Zr
      5. SS 304[a]
      6. Niobium

(a) Contained a $\frac{1}{2}$ mil thick vanadium
    barrier foil.

Fuel: U-20% Pu-10% Fs

Heat Transfer Medium: Na

Reactor Power Output: 6, 497, 045 kwh

Top Section:

    Specimen Cladding (Individually unidentified)

1. Nb-1% Zr
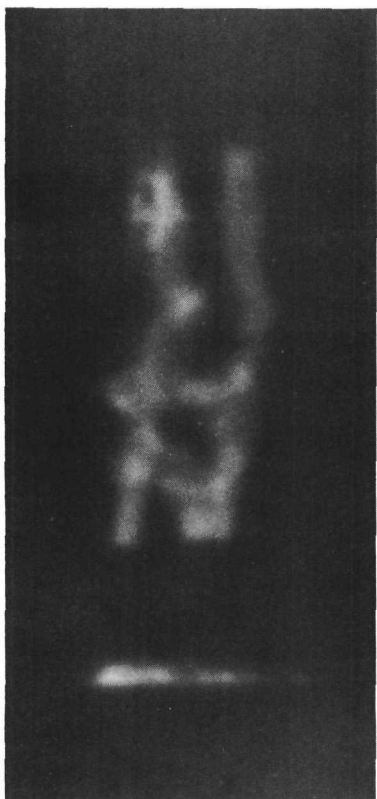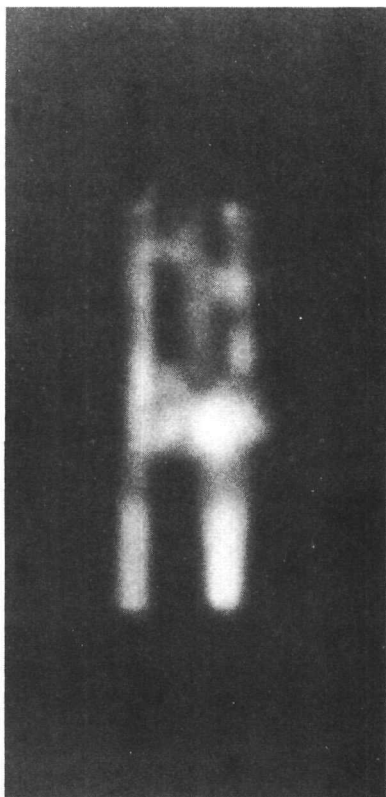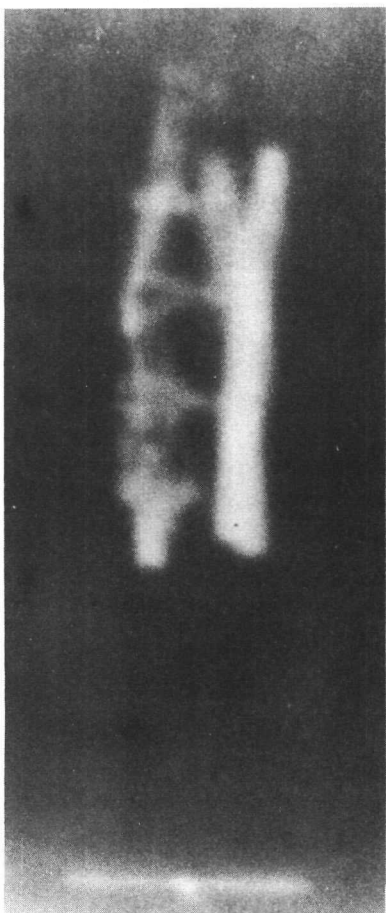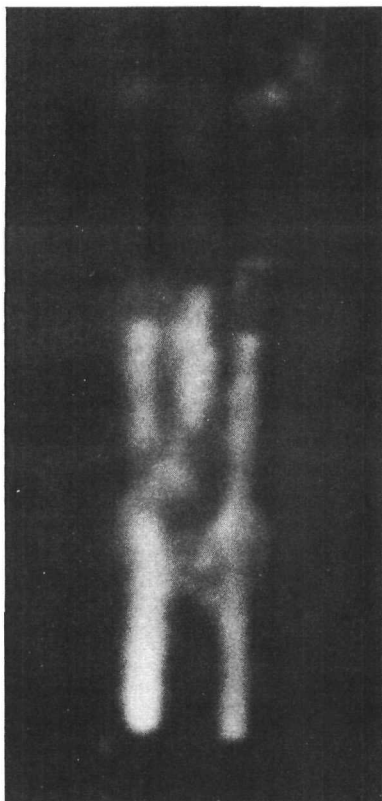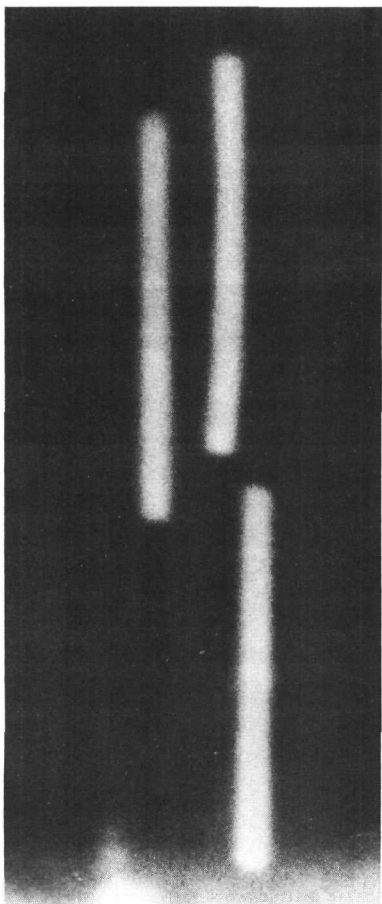2. Niobium
3. Vanadium

Figure 14

Autoradiograph of Capsule CP-18.

Bottom Section:

    Specimen Cladding (Individually unidentified)

4. Nb-1% Zr
5. Vanadium
6. SS 304[a]

(a) Contained a $\frac{1}{2}$ mil thick vanadium barrier foil.

The origin of the stresses may possibly be found in the freezing and melting of the sodium with the off-on cycles of the reactor. Preparations are being made to open the capsules for a detailed examination of the contents.

4. Nondestructive Testing

a. Ultrasonic Techniques - Lamb wave experiments on thin wall, small diameter tubing has been started. The test pieces are Type 1100 aluminum with 0.030 in. wall and 0.5 in. O.D. Lamb waves and shear waves were used to detect O.D. transverse flaws of 0.002 in. widths and with depths varying from 0.002 in. to 0.009 in. These are easily detected dynamically and the amplitude of the response is approximately the same whether the angle of incidence is that necessary to generate shear or Lamb waves. The reason for this, it is postulated,is that in testing for O.D. defects the phenomenon utilized is neither shear nor Lamb waves but a direct reflection from the defective surface.

The sensitivity of any test of this type is limited by the surface condition of the specimen. The aluminum tubing used is ordinary stock tube which has been polished with oil and steel wool but nevertheless it is a soft material and the specimens contain pits and surface scratches of the order of magnitude of 0.002 in. It is impossible to find defects smaller than this.

The signal response to I.D. defects is much less than for O.D. defects. The noise level is such that the smallest defect that has been found dynamically is approximately 0.003 in. - 0.004 in. In all the tests conducted on I.D. simulated defects, however, the received signal due to a Lamb wave mode has been much greater than with shear waves and some defects whose response is near the noise level can be detected by Lamb waves and not by shear.

To decrease the noise level, tubing is being prepared with an optical finish. Tests will be conducted on these to determine how small a defect can be detected under these rather ideal conditions.

b. Neutron Techniques - Gadolinium screens, have been studied in regard to thickness for best speed in both a double and a single screen technique. The screens available are in the thickness range of 0.00025 in. to 0.002 in. For single screen use, the screen thickness which produces the best speed is in the order of 2 mils. The best speed results for the double screen technique has been found for a front screen (toward the neutron source) thickness of 0.0005 in. and a back screen thickness of 0.002 in.

Although sharpness versus screen thickness studies are still in progress, two preliminary conclusions concerning image sharpness can be drawn. First, the use of a gadolinium single screen back of the photographic film (back screen) produces the best image sharpness of any of the neutron

photographic methods studied, including those made by transfer techniques. Second, the use of the film toward the source produces better speed and better image sharpness than when the gadolinium screen is between the source and film (at least for thicknesses 0.00025 in. and greater).

Gadolinium appears to possess all the qualities desired of a direct exposure metal screen material. Its tendency to become radioactive (for naturally occurring material) is negligible, meaning that additional transfer time after the neutron exposure is unnecessary and that there is little, if any possibility of "double exposures," in using the same screen for two consecutive pictures. More important, the material has a very high thermal neutron cross section (46,000 barns) so that it can be used with good speed in the small thickness mentioned here.

A single gadolinium screen, 0.002 in. in thickness, has a speed rating comparable to that of cadmium and rhodium, the materials which have yielded the best speed for single metal screen used up to this time. Another important factor, particularly for the good sharpness obtained, is that much of the film exposure appears to be due to relatively soft radiation. This fact is consistent with data in the literature and has been confirmed here by comparing the film densities obtained on multiple film exposures with gadolinium screens.

c. <u>Eddy Current Techniques</u> - Development work has been reopened on the pulsed field-reflection system last reported in January, 1961 (ANL-6307). This electromagnetic test method replaced the sinusoidal currents and test coils or probes of our older eddy current test system with pulsed fields emanating from small apertures in special masks. Test information about the metallic specimen being examined is received as a series of reflections from the surface and from inside the metal.

This system represents a possible new approach to the problems of the electromagnetic testing field. Recently it was discovered that the pulsed-field reflection system in its present form possesses a pronounced sensitivity to the orientation of any possible flaw in the metal passing under the aperture.

The mask-aperture-pickup assembly can be oriented to achieve maximum pickup of defects of one orientation while minimizing all others. This is important because a set of mask-aperture-pickup assemblies inspecting a test specimen containing defects could obtain more extensive information about defect size, depth, orientation and frequency of occurrence than has been obtained with other more conventional test systems. Additional experiments are being undertaken so that a better understanding of this effect can be achieved.

C. Reactor Materials Development

1. Radiation Damage in Steel

a. Theoretical Model - A set of multigroup cross sections has been adapted for the DSN Code which will give a detailed spectrum at neutron energies greater than 0.1 Mev. Flux calculations with these cross sections are being made for the EBWR pressure vessel wall and the location of sample cans at the outer edge of the core. The latter will be compared with foil measurements. A trial set of foils was exposed and then removed from EBWR to check handling and counting techniques. New foils will be inserted before the next period of EBWR operation. Calculations are also planned for MTR sample locations and the BORAX-V pressure vessel wall.

b. Magnetic Properties - Attempts were made to obtain coercive force measurements on samples of irradiated SA-212-B material. These measurements were initially attempted in a high level β-γ cave with steel walls. However, the measurements had to be abandoned after it was discovered that the high intensity magnetic fields uncontrollably magnetized the steel walls and structure of the cave. The coercive force meter was reassembled elsewhere in an area free of interfering concentrations of iron and steel. Measurements of the coercive force were then completed on the 34 as-irradiated samples described in the Progress Report for July, (ANL-6399, page 57).

It was found that the coercive force of the as-irradiated steel was relatively unaffected by the irradiation, although the mechanical hardness increased. At the lowest exposure, (Group I, 1×10^{20} nvt greater than 1 Mev, as reported by the MTR staff), the coercive force was 3.5/4.0 oersteds - about the same as fully annealed unirradiated material. At the highest exposure, (Group IV, 2.8×10^{21} nvt greater than 1 Mev), the coercive force was slightly lower, about 3.1/3.8 oersteds. The intermediate Group II and Group III specimens were between these values and generally consistent with the trend, i.e., a gradual magnetic softening with increasing dosage.

Each of the groups was represented by a minimum of eight samples. Forward and reverse magnetic polarity measurements of the coercive force were made on each bar. The maximum deviation found per bar was 0.1 oersteds which was the limit of the accuracy of the measurements with the unstabilized voltage power supply to the instrument. The reproducibility of the measurements was also found to be 0.1 oersted. Measurements of the hardness and coercive force of thermally heat-treated irradiated bars (900°F anneal for 1, 2, and 3 hours, respectively) are in progress.

c. Micrographic Examination of Steel - The cooperative program between the U. S. Steel Corporation Applied Research Laboratory and ANL for the metallurgical examination of the as-irradiated and post-irradiation thermally heat-treated SA-212-B EBWR pressure vessel steel from the ANL-26 irradiation was concluded (see Progress Report, December, 1960, ANL-6295, p 50) with a review of the 15,000X photomicrographs. The photos showed that there were no observable differences between unirradiated, irradiated, and the post-irradiation thermally heat treated structures. Weld metal and heat affected zone areas were likewise unaffected by irradiation. All four groups of the ANL-26 irradiation were represented in the investigation.

D. Reactor Component Development

1. Development of Viewing Systems.

Charge Storage in Glass - Additional studies have been made of the charge displacement that occurs in irradiated glass when the glass is subsequently heated, the thermoelectric effect (seeProgress Reports for December, 1960, ANL-6295, p 53; June, 1961, ANL-6387, p 56). The effect is believed to be caused by energetic secondary electrons originating outside the glass sample. The stability of these trapped electrons have been determined by holding "cabal" glass samples at $25°$ and $100°C$ for varying times after irradiation before measuring the thermoelectric effect. It has been found that the stability of these trapped electrons is very similar to the stability of the color centers produced by gamma radiation. It is planned to extend these tests to glasses containing cerium.

2. Development of Manipulators for Handling Radioactive Materials

Transistorized Servo System for Master-Slave Manipulator - A servo system has been developed for use in a 50-lb capacity master-slave electric manipulator similar to the ANL Model 3. The system has been improved over the previous vacuum tube system both by the use of transistors and by circuit changes. The improvements due to the use of transistors instead of vacuum tubes are: the elimination of hazardous high voltage supplies, the reduction of heat dissipation by the amplifier and possible longer service life.

Circuit improvements include a positional data system operating at 6 kc which reduces the number of leads between master and slave drive units and eliminates previous difficulties with noise and oscillation in a 60-cycle system caused by pickup in the electrical cables. This new system has a d-c positional signal which is biased so that open circuit failure can be detected. Hence, the "fail-safe" circuit which sets the brakes on the slave drives will function for almost all types of electrical failures.

The system has been designed with considerable amounts of feedback in the voltage and power amplifiers sections in order to achieve gain stabilization. This results in a system which is insensitive to changes in transistor characteristics due principally to temperature effects, and which allows quick change of components. For example, the over-all amplifier gain was found to change by only 4 percent for an ambient temperature change from 20° to 44°C.

The system also includes the other functions included in the previous system. The operating time at full capacity is extended by automatically switching the fixed field excitation of the servomotors from partial power to full power when required. The operator can select a suitable master-to-slave force ratio, so that the forces exerted by the slave arm are either equal to, or three times, the forces at the master arm.

E. Heat Engineering

1. Double Tube Burnout Study

The double tube burnout test is designed to provide constant steam quality burnout data. With a constant exit quality the hydrodynamic characteristics should remain unchanged during the burnout, and the flow transients, which have been observed in many burnout tests, should be eliminated.

The test section, as described in the June, 1961 Progress Report (ANL-6387, page 56) requires two independent power supplies, a power control system that will give a constant total power from the two supplies, and two burnout detectors. The wiring of the power control system has been completed. The second burnout detector was completed and tested and is ready for use. A flow measurement orifice was installed and has been calibrated in place.

The test section was completed but a radiograph of the assembly revealed the inner tube was badly bowed because distortions occurred during the final weld. The test section was partially rebuilt, and changes in the assembly procedure corrected the problem of bowing.

During a hydrostatic test of the repaired test section, leaks were observed in the weld joining the Inconel-X outer tube and the stainless steel flange. Attempts to seal these leaks resulted in progressive cracking in the Inconel-X tube. The tube finally failed completely. The test section is being rebuilt.

2. High Temperature Liquid Metal Meeting

A classified meeting was held June 14-15, 1961, at Argonne National Laboratory to discuss problems and experimental programs pertaining to high temperature liquid metals. The meeting was attended by personnel from industry, National Laboratories, NASA, and the AEC. Proceedings are now being prepared.

3. Hydrodynamic Instability

The frequency-dependent behavior of a boiling natural circulation loop was obtained at three frequencies of power oscillation for comparison to analog model hydrodynamics. Downcomer restriction influences on the inception and behavior of instability were investigated for the 1.6-cm inside-diameter test section and riser. Tests were completed for two values of restriction at 41 atm (600 psig) and at various heat fluxes.

4. Boiling Liquid Metal Experiment

The small scale loop designed for measurement of vapor volume fractions and two-phase frictional behavior of flowing alkali metals has progressed to the assembly stage. The sheathed platinum/platinum - 10% rhodium thermocouple assemblies were found to have defective welds and have been returned to the vendor for replacement.

The low temperature NaK-argon loop operated successfully for 150 hours before oxide fouling necessitated shutdown. Cleaning has been completed and the loop is now back in operation. The electromagnetic flowmeters have been calibrated against a standard orifice at NaK temperatures up to 180°C. Some two-phase, two-component flow data have been taken which indicate that accurate volume fraction measurements can be obtained using 2 em flowmeters in series, at least in the low void region, i.e., less than 40%. Higher void fractions will be investigated. These voids are substantiated by the one-shot gamma-radiation technique used in air-water and steam-water flow studies. The simplicity of void measurement (if accurate) by the use of this type of flowmeter offers several promising applications.

5. Heat Transfer in an Annulus

In support of the proposed TREAT experiments with fast reactor fuel pins, heat transfer studies leading to the prediction of temperature distribution of the coolant flowing in an annulus and heat transfer coefficients have been undertaken. This information is required for prediction of the temperature distribution and the condition at which the failure of the fast reactor fuel pins occurs.

The steady state laminar flow problem of heat transfer in an annulus with unsymmetrical heating has been formulated, and the problem has been reduced to the solution of a Sturm-Liouville type equation for the eigenvalues and eigenfunctions. The eigenfunctions of this equation give the radial temperature distribution. The first six eigenvalues and eigenfunctions have been computed on the analog computer. Results have been obtained for several values of the ratio of the inside to the outside radii of the annulus.

Heat transfer coefficients and Nusselt numbers have been calculated for the entrance region. Nusselt numbers have also been computed for the region where fully developed temperature profile exists.

6. Heat Conduction in the Axial Direction

a. Streamwise Conduction - Computations have been completed in connection with determining the relative importance of some assumptions made in the solution of the heat conduction by liquid metals flowing between parallel plates. Specifically, it was desired to examine the influence of axial surface heat flux density function on Nusselt number for low Prandtl number coolants. Calculations were made both neglecting and including streamwise conduction (in the plates). The analysis is still to come, but it can already be concluded that the streamwise conduction term in the heat conduction equation can be neglected except in very extreme cases.

b. Effect on Nusselt Number of Axial Heat Variation - Solutions were obtained for uniform (step) and cosine surface flux function inputs. Since the solved equations are linear, an attempt was made to apply the Duhamel superposition theorem using the step function results to match the calculated cosine function results for Nusselt number as a function of position. Calculation of several points on this basis indicated an excellent match. This application agrees with that of V. I. Petrovichev.* This technique was also used by W. B. Hall and P. H. Price** for gas as a coolant. These resulted in similar curves (however, the Stanton number was plotted as a function of axial position) for the sine distribution, and further noted that the shape of the curves should be the same for the uniform and exponential distributions, merely resulting in different magnitudes for the Stanton number. Their use of the Duhamel superposition procedure started with experimentally obtained curves for the uniform flux distribution and therefore required no consideration of the axial conduction term. It might prove to be true that calculation of the uniform case is all that is necessary for most systems, and that regular application of the Duhamel theorem will suffice for other axial flux distribution functions. At any rate the influence of the flux function on Nusselt number appears to be quite significant and is not to be ignored.

---

*V. I. Petrovichev, "Heat Transfer to Mercury in a Circular Tube and Annular Channels with Sinusoidal Heat Load Distribution," International Journal of Heat and Mass Transfer, Vol. 1, Nos. 2/3, August, 1960.

**W. B. Hall and P. H. Price, "The Effect of a Longitudinally Varying Wall Heat Flux on the Heat Transfer Coefficient for Turbulent Flow in a Pipe," International Heat Transfer Conference, Univ. of Colorado, Boulder, Part III, p. 607, forward (Preprint).

F. Separations Processes

1. Fluidization and Fluoride Volatility Separations Processes

The volatilities of uranium and plutonium hexafluorides are the basis of schemes being considered for reprocessing power reactor fuels. Emphasis is now on the development of the Direct Fluorination Volatility Process applicable to the processing of typical oxide fuels.

The direct fluorination of high-density, sintered uranium dioxide pellets in an inert bed of fluidized solids is being investigated to study problems of heat removal, reaction rate, fluorine utilization efficiency, and general behavior of the system.

Processes for recovering uranium from zirconium-enriched uranium alloys are being developed. Use of hydrogen chloride for zirconium removal and decladding followed by direct fluorination of uranium is being tried. These reactions are conducted in fluidized beds of inert solids (currently Norton "Alundum") which serve as a heat transfer medium.

The fluorine chemistry of plutonium and uranium is being investigated in order to obtain information useful in establishing process flow-sheets as well as information of a more fundamental nature. Laboratory fluorinations of solid solutions of uranium-plutonium dioxides mixed with inert solids are being carried out. Pure crystalline aluminum oxide, which has been shown to be the best inert solid of those tested, is currently being used.

a. <u>Direct Fluorination of Uranium Dioxide Fuel</u> - The variables currently being studied in the direct fluorination of uranium dioxide pellets are temperature and fluorine concentration. Oxygen concentration is also a variable because oxygen produced during the fluorination increases the reactive surface area. In order to minimize the retention of plutonium and uranium on the fused alumina fluid-bed material, it appears desirable to operate at less than 450°C. Previously, comparative rates were obtained at temperatures from 350° to 500°C in shallow bed tests with and without oxygen present in the fluorine. In the present period, the fluorination of a six-inch deep bed of uranium dioxide pellets in alumina was carried to completion at 400°C in the presence of recycle oxygen (average fluorine concentration 16 percent). In 11.0 hours 86 percent of the 4.4 kg charged was recovered as uranium hexafluoride product with an overall fluorine utilization efficiency of 83 percent. While this batch reaction time is not prohibitively long, equivalent recovery has been achieved at 500°C in about 4 hours. It is believed that higher rates can be obtained at 400°C by increasing the fluorine concentration. Further studies of processing conditions are planned to determine the role of oxygen on overall fluorination rate, to demonstrate close temperature control over a wider range of reaction rates, and to determine conditions for optimum fluorination of the pellet residues at the end of a batch reaction.

b. Halogenation Studies on Uranium-Zirconium Alloys - Packed beds of Norton "Alundum" are being evaluated as filters for retaining uranium chloride particulate formed during hydrochlorination of the low uranium-zirconium alloy and entrained by the volatile zirconium tetrachloride. A mixture of hydrogen chloride-nitrogen was passed into a 1.5-in. diameter fluidized reaction zone. The reaction products then passed into a three-inch diameter bed filter and the gases passed to the off-gas system, a zirconium tetrachloride condenser followed by a water scrubber. Filter-bed conditions were as follows: superficial gas velocities of 0.14 to 0.28 ft/sec, -40 +200 or -20 +36 mesh particles Alundum, and temperatures of 375° to 425°C. The alloy charge to the reaction zone ranged from 4.1 to 7.6 grams of uranium contained in a 2.7 weight percent uranium-zirconium alloy. Initial results indicate that better filtration is achieved by using (1) low velocities, (2) down-flow of the gas through the packed bed rather than up-flow, and (3) small particles. Uranium losses to the off-gas system ranged from 0.3 to 0.6 percent of the uranium charged.

c. Fluoride Separations - In ten-hour fluorinations at 500°C of solid solutions of uranium-plutonium dioxides mixed with crystalline alumina the removal of plutonium and the concentration of plutonium remaining on the alumina were intermediate to those found in previous ten-hour fluorinations at 450° to 550°C as shown by the following:

Temp (°C)	Percent Plutonium Removal	Concentration of Plutonium in Residual Alumina (%)
450	98.5	0.03
500	97.0	0.05
550	96.0	0.07

Several ten-hour fluorinations of solid solutions of uranium-plutonium oxides at 450° and 550°C were carried out with a gas mixture containing 25 percent oxygen in fluorine. The presence of the added oxygen did not adversely affect the removal of plutonium.

The use of the bed material for the fluorination of more than one batch of fuel has been considered. In order to determine how the quantity of plutonium residue in the alumina varies with reuse of the solid, a series of fluorination experiments was performed using the residual alumina in successive ten-hour fluorinations at 450°C. Starting with an initial concentration of about one percent of plutonium in the alumina for each fluorination reaction, a residual value of 0.029 percent plutonium was obtained after the first fluorination and a value of 0.1 percent was obtained for each of the four subsequent experiments in which the alumina was reused.

The kinetics of the nickel-fluorine reaction has been studied from 100° to 700°C. Isothermal rates have been obtained at 100°C degree intervals. No fluorine pressure dependence, in the range 100-700 mm, was

noted at 500°C in which the nickel fluoride film thickness ranged from
7×10^3 Å to 1.5×10^4 Å. However, a pressure dependence in the same
pressure range was noted at 600°C for fluoride scale thicknesses of about
2.5×10^5 Å. The rates obtained are an order of magnitude greater than the
values obtained at Oak Ridge (AECD-4292) at 600°C at which temperature
the workers at Oak Ridge also obtained a pressure dependence.

2. General Chemistry and Chemical Engineering

The attainment of lower cost nuclear power depends on the develop-
ment of more economical methods of manufacture of nuclear fuel materials.
Research and development for devising new chemical methods or improv-
ing chemical engineering techniques or equipment is being conducted.

The fluid-bed conversion of uranium hexafluoride into uranium
dioxide is an alternative method for the production of enriched oxide for
nuclear reactor fuels. The process involves either a single-step pyrohy-
drolysis and reduction using steam and hydrogen simultaneously, or a two-
step process using alternatively steam or hydrogen, followed by the other
reactant.

Conditions for liquid metal reduction of the oxides of uranium, plu-
tonium, and thorium are being explored. Preparation of refractory uranium
and plutonium compounds is being investigated.

a. Conversion of Uranium Hexafluoride to Uranium Dioxide - Two-Step Fluid-Bed Process

(1) Steam Hydrolysis of UF_6 to UO_2F_2 - Three runs totalling
31 hours were made in the three-inch diameter reactor for the preparation
of uranyl fluoride by the steam hydrolysis of uranium hexafluoride. Operat-
ing conditions were as follows: superficial gas velocities ranged from
0.45 to 1.0 ft/sec (200 and 330 percent excess steam) and seed recycle rate
from 14 to 24 percent, 100 g/min uranium hexafluoride feed rate, 18-in. bed
height and 200° to 230°C bed temperature. Stable bed behavior was demon-
strated over this range of operating conditions. The greatest change effected
was a reduction of about 25 percent in the average bed particle size with the
high recycle rate in use over a period of ten hours.

(2) Reduction of UO_2F_2 to UO_2 - A series of four-hour batch
experiments at 650°C using 50-50 mixtures of steam and hydrogen and flu-
idizing gas velocities in the range 0.6 to 2.0 ft/sec was made to determine
the overall conversion to uranium dioxide of three-kilogram batches of
uranyl fluoride. The fluidizing velocity had little effect on conversion;
specification-grade material (< 200 ppm fluoride) was achieved in all cases.
Relatively good results (350 ppm residual fluoride) in a static-bed experi-
ment conducted at 0.2 ft/sec (minimum fluidizing velocity of the bed was
0.25 ft/sec) indicate the possibility of using a deep, moving-bed system for
this step.

Monel corrosion coupons exposed to column conditions for 50 hours showed corrosion equivalent to 1.2 mils/mo for samples located in the bed and 1.7 mils/mo for samples in the gas phase above the bed. These data confirm corrosion rates obtained previously.

b.   Liquid Metal Reduction Studies - In the reduction of thorium dioxide by zinc-5 weight percent magnesium alloy, a minimum magnesium concentration of about 35 mole percent of the cations in lithium chloride-magnesium chloride-magnesium fluoride fluxes was necessary to achieve satisfactory reductions.

c.   Preparation of Uranium Carbide - An attempt has been made to prepare uranium carbide by reaction of hydrocarbon gases with uranium in zinc-magnesium systems. Methane and acetylene were each contacted with uranium in a zinc-11 weight percent magnesium solution at 800°C but little uranium carbide was produced in these experiments.

3. Chemical Metallurgical Process Studies

Continued progress is being made in the development of new pyrometallurgical methods for reprocessing nuclear reactor fuels and in the refinement of processes which are in advanced stages of development. Supporting studies are providing physicochemical data on liquid metal systems of process interest and thermochemical data on materials of interest to high-temperature chemistry. Solubilities of fissionable and fission product elements in liquid metal solvents are being measured. Phase studies of the uranium-zinc and uranium-magnesium-zinc systems are providing information of direct importance to the pyrometallurgical processes that will be used in the EBR-II fuel cycle. Studies of the distribution of elements between immiscible liquid pairs are also yielding information of process interest. Thermodynamic functions for elements in liquid metal solvents and for the more important solid intermetallic phases are being evaluated. Studies which are being made with the recording effusion balance for phase diagram investigations are providing useful information concerning binary systems in which one component is volatile. Both oxygen and fluorine bomb calorimetry are being used to provide basic information.

a.   Liquid Metal Solvent Studies - The solubility of scandium in liquid cadmium (reported in the June, 1961, Progress Report, ANL-6387) indicated a peritectic transformation at about 420°C. The existence of the transformation has been confirmed by thermal analysis of a 3 weight percent scandium-cadmium ingot which, on heating, yielded an arrest at about 414°C. The scandium-cadmium intermetallic phase in equilibrium with the saturated liquid phase above the peritectic temperature has been identified as $ScCd_3$. Work is in progress to characterize the intermetallic phase below the peritectic temperature.

The solubility of uranium in liquid thallium may be represented by the empirical equation

Uranium (400° to 850°C): $\log(\text{atom percent}) = 4.45 - 5940\ T^{-1}$.

The distribution coefficient of cerium between the partially miscible liquids lead and zinc has been remeasured at several temperatures. The values of the coefficient (weight percent of cerium in zinc/weight percent of cerium in lead) were found to be 18.7 at 651°C, 8.1 at 704°C and 5.0 at 736°C. These values are slightly lower than the values that were reported in the November, 1960, Progress Report, ANL-6269.

The uranium-indium system has been studied by means of the galvanic cell method. The free energy of formation of UIn_3 over the temperature range of 353° to 675°C may be represented by the equation

$$\Delta F_f^\circ = -24{,}670 + 8.377\ T + 3.344 \times 10^{-3} T^2$$

where ΔF_f° is the free energy of formation (cal/mole) of UIn_3 formed from solid uranium and liquid indium. The activity coefficient of uranium in saturated indium solutions varies from 0.55 at 400°C to 1.4 at 700°C.

A galvanic cell is being constructed for the study of the plutonium-zinc system.

The lanthanum-zinc and praseodymium-zinc systems have been studied by measuring the decomposition pressures as a function of composition by means of the recording effusion balance. Phases of the following apparent compositions have been found: (1) in the lanthanum-zinc system, $LaZn_{12}$, $LaZn_8$, $LaZn_{6.6-7.2}$, $LaZn_{3.8-5.6}$, $LaZn_2$, and $LaZn$; and (2) in the praseodymium-zinc system, $PrZn_{11}$, $PrZn_{8.5}$, $PrZn_{6.9-7.4}$, $PrZn_{3.4-5.6}$, $PrZn_2$, and $PrZn$. Data concerning the cerium-zinc system have been previously reported (in the October and November, 1960, Progress Reports, ANL-6253 and ANL-6269).

Further studies of the uranium-zinc system indicate that the lower equilibrium limit of the delta phase ($UZn_{8.5}$) in the presence of free uranium is between 550° and 600°C and is probably very close to 550°C.

The dependence of the relative partial molal enthalpy of various solute metals at high dilution in liquid cadmium on the cohesive energy density ($\Delta H_{vap.}/V_{atomic}$) has been found to divide the solutes into three classes: (1) the meta-metals (such as zinc, indium, thallium, and lead) and semi-metals (such as gallium, tin, antimony, and bismuth), where the completely filled d-orbitals do not significantly contribute to bonding, partial molal enthalpies are small (about 1 kcal) and positive; (2) copper, silver, and gold, where the first filled d-orbitals probably make some contribution to the bonding; with these solutes, the partial molal enthalpy passes through

a minimum; and (3) the transition metals, where the incompletely filled d-orbitals make significant contribution to the bonding, the partial molal enthalpies of these elements increase rapidly with cohesive energy density.

The excess partial molal entropies of metallic solutes at high dilution are divided into two main classes depending on the radius of the solute. The first class, which includes those elements whose radii lay in the interval of 1.40 to 1.75 Å (i.e., within ± 15 percent of the radius of cadmium, 1.54 Å), have excess molal entropies within a few entropy units of zero. Silver, the meta- and semi-metals are included in this class. The second class consists of copper and the 3-d transition metals. The radii are 1.3 Å or less. The excess entropy rises from -9.4 entropy units to +3.1 entropy units for a decrease in radius of only 0.5 Å.

b. <u>Calorimetry</u> - Preliminary values of 8196.6 $\pm$ 1.8 cal/g and 2593.1 $\pm$ 0.5 cal/g have been obtained for the heats of formation of titanium and hafnium tetrafluorides, respectively.

A value of 8534.1 $\pm$ 1.7 cal/g has been obtained for the heat of combustion of boron nitride in fluorine. It has been found that the reaction of boron with ClF_3 gives a complex mixture of products.

Preliminary results indicate that there is a measurable difference between the heats of combustion of ZrH_2 and ZrD_2 in oxygen.

A method of igniting a benzoic acid pellet without the use of a cotton fuse has been devised. The pellet is ignited by contact with a one-mil platinum wire which is electrically heated.

G. Advanced Reactor Concepts

1. Fast Reactor Test Facility (FARET)

The engineering and physics parameters for an experimental facility to test advanced fast reactor cores are being examined to prove the feasibility of a generalized test device.

A reference core has been selected as the nucleus for preliminary design studies that will define the remainder of the facility. Some specifications for this core model are UC_2 fuel elements, an exit sodium temperature of 1400°F and a gross heat output of 50 Mw. Thus, the FARET facility will be capable of thermal conditions that represent a significant advance over current fast reactor practice.

Preliminary design of a pressure vessel suitable for the specified temperature has been completed. It appears that Type 316 stainless steel will be an adequate material if care is taken to limit stress from gamma heating. The neutron and gamma flux distributions for a 40-cm radius core

(500 liter) with a 40-cm reflector were calculated from EBR-II multigroup flux data. From these the thermal stress in the pressure vessel wall was estimated to be about 4000 psi. With a bypass flow of sodium coolant between the thermal shield and vessel, the maximum vessel wall temperature can be limited to 1100°F. At this temperature, the permissible working stress for Type 316 stainless steel safety exceeds the calculated thermal and hydraulic loads.

It appears that the reactor vessel temperatures should be kept as low as practical and calculations are underway to estimate the amount of core bypass flow needed to maintain various maximum temperatures. As a starting point in a study of the heat transfer loop requirements it was decided to investigate gravity flow from the reactor discharge to the main coolant pump as a means of minimizing pressure seal problems at the reactor vessel head. Pressure losses in the lines have been estimated and efforts are underway to specify an intermediate heat exchanger which would be compatible with the available head of primary sodium.

Biological shielding requirements for 50-Mw operation were also obtained from the flux data. Approximately 150 cm of concrete plus 20 cm of borated graphite will be needed axially. In the radial direction, an extra 10 cm of borated graphite is required.

2. Direct Conversion Survey for Mobile Systems

As a first approach to find new ways to use nuclear energy for surface transportation, reactors for the production of chemical fuels suitable for either internal combustion engines or fuel cells are being considered.

A survey has been made of the energy storage capacity of the various light elements and light element compounds (mainly hydrides) up to potassium in the periodic table. The materials considered as oxidizers for these elements were fluorine, oxygen, and nitrogen. For terrestrial transportation missions, there is a decided weight advantage if air is the oxidizer; hence, light element oxides and nitrides are of particular interest, with the oxides favored because of their higher heats of formation. Table X gives the energy storage capacities of light elements and compounds competitive with gasoline. For use with these fuels, the following types of converter-regenerator cycles have been considered:

(1) Heat engine - discard reaction products.

(2) Heat engine - save and regenerate reaction products.

(3) Fuel cell - save and regenerate reaction products.

Table X. Energy Storage Capacities of Light Elements and Compounds

Compound or Element	Weight, kcal/gm	Volume, kcal/cm^3	Volatile Combustion Products
Gasoline	10.4	6.49	yes
H_2	28.9	2.05	yes
B_5H_9	17.0	10.4	no
Be	16.1	29.8	no
B	13.9	32.4	no
Li	10.3	5.30	no
LiH	9.74	7.59	no
PH_3	7.90	5.89	yes
C	7.83	15.7	yes
Al	7.39	20.0	no
Si	7.20	14.4	no
Mg	5.91	10.3	no
P	5.81	10.6	yes
H_2S	3.63	3.63	yes
NaH	2.69	3.77	no
S	2.21	4.52	yes

For the first type cycle it is required that the oxidation products be readily exhausted, i.e., volatile, and that the fuel be readily synthesized from relatively abundant materials. As seen from the above table, H_2, PH_3, P, H_2S, and S are possible candidates for this type of cycle. Theoretically, all of the remaining materials listed are possibilities for Cycles 2 and 3.

In considering possible regeneration cycles for the light element oxides, it is found that most of the thermal reduction processes in use today depend on carbon as the reducing agent. Even the electro-refining processes in use today depend on carbon as the reducing agent. Even the electro-refining of aluminum consumes about two-thirds pound of carbon per pound of aluminum produced. Electrolysis of water to produce hydrogen and oxygen is one process that does not use carbon. Typical energy efficiencies of commercial electrochemical processes are 60% (electrolysis of water) and 40% (refining of aluminum - not including carbon consumed).

A survey of some intermetallic compounds for which thermochemical data are available indicates that their heats of formation are considerably lower than for the formation of oxides; however, so far data on really light element intermetallics have not been located.

3. Research and Test Reactor Design

The potential advantages of a D_2O reflector for a light water moderated, flux trap core are being explored as part of a search for improved research reactor concepts. A core design with a heavy water reflector

contained in a low pressure region (1 atm) is being used for an analytical model for these studies. In this design, the pressure vessel would be located between the reflector and the core. A series of calculations showed that the total (thermal and pressure) stresses in the wall of a steel vessel would exceed the design limit while the stresses in an aluminum wall would be about equal to the design limit. It is felt that a $\frac{1}{2}$-in. to $\frac{5}{8}$-in. thick, specially designed aluminum annulus (such as a honeycomb structure) could be used for a pressure vessel. Possible designs for such a vessel will be investigated. Also, the flux distribution and energy spectrum with a D_2O reflector will be compared to those with a beryllium reflector.

4. High Power Density Reactors

A thermodynamic analysis of various high temperature cycles for central station application is underway. The objective of this study is to screen the exotic cycles for the economic incentives that they may offer in comparison with an advanced conventional plant. Some of the systems which will be investigated are given in Table XI.

Table XI. Various High Temperature Systems to be Studied

Reactor Coolant	Primary Turbine Fluid	Secondary Turbine Fluid	Heat Rejection
Boiling Sodium	Sodium	Potassium	Process Steam
Boiling Sodium	Sodium	Mercury	Process Steam
Liquid Lithium	Sodium or Potassium	Mercury	Process Steam
Boiling Sodium	Sodium	H_2O	-
Liquid Sodium	Sodium or Potassium	H_2O	-
Liquid Potassium	Mercury	H_2O	-

5. Supercritical Water Reactor

A study of supercritical reactors is being performed with the following objectives:

(1) To determine the maximum power capability of a supercritical water-cooled reactor core in a pressure vessel.

(2) To review the present state of supercritical water technology as it pertains to nuclear reactors.

The power output of a supercritical water reactor is a function of the power density and the maximum size vessel that can be manufactured. Information is being obtained on the maximum size of vessels currently obtainable. In the interim, the reactor power density limits consistent with reasonable turbine throttle temperatures and pressures will be determined.

6. Direct Conversion Studies - Cesium Plasma Diode

a. Magnetic Effects - The effect of magnetic fields on the cesium plasma diode was investigated. Through a sapphire window and a blue Wratten No. 98 filter the cesium plasma flow was observed visually to be displaced in the direction predicted for the E x B plasma drift. The electrodes were in parallel plate geometry with a separation of 0.375 cm. The UC:ZrC electron emitter patch was 0.635 cm in diameter mounted on a tantalum backing and facing a copper collector of equal diameter with a wide guard ring. The cesium pressure was 3 x 10^{-3} millibars.

On the application of a magnetic field of 23 gauss parallel to the plates and in the direction of observation the plasma was displaced perpendicular to the direction of observation. At the same time the collector short circuit current decreased from 1 ampere to 0.5 ampere and the guard ring short circuit current increased from 2.8 amperes to 3.0 amperes. This displacement of the electron current from the collector to the guard ring confirms that the observation of the flow displacement indicated an actual movement of plasma.

b. Performance - A method to fuse slices of uranium-zirconium carbide to a tantalum button is under development. These slices, which have a thickness of about 0.025 to 0.05 mm, are deposited on a tantalum button and fused to it by induction heating or electron bombardment. A diaphragm with a tantalum button coated with $UC_{0.03}$-$ZrC_{0.07}$ by this method was used to measure electron emission and work functions in a cesium plasma cell, as described in previous Progress Reports. The area of the emitter was about 0.317 cm^2. The collector of the same area was surmounted by a guard ring. The collector and guard ring were connected and operated as a single electrode, so that practically the total emitter current was collected, except for those electrons reflected back or absorbed in the plasma. The emitter-collector distance was approximately 1.2 mm. Applied voltages between emitter and collector were varied from -4 to +6 volt. Voltage-current graphs were plotted for temperatures varying from about 1400°K to 2200°K for each series. The procedure was then repeated for increasing cesium pressures.

In addition, the power density was plotted against the voltage, and the power maximum was marked. From the expressions developed by W. Nottingham the approximate values of the mean free path "λ" and the cesium atom density were calculated. The cesium ion density will be about one-half of this value, if the work function of the contact material exceeds the cesium ionization voltage of 3.81 volt. For low cesium pressures, or λ less than the emitter-collector distance, the electrons travel essentially without collisions and the space charge is neutralized, if the ion density exceeds somewhat the electron density. The currents at zero-applied voltages are the saturation currents, if a further increase of voltage leaves

the current constant. In Fig. 15, the current densities are shown on a semi-log scale as functions of emitter temperature, for four ranges of cesium pressure. The λ's were considerably larger than the electrode distance. For the lowest range of cesium pressure, Fig. 15 shows that at high temperatures the current increase is very low. The cesium ion density is no longer sufficient to neutralize the space charge. Figures 16 to 18 show I/T^2 plotted against ϵ/KT, (ϵ = electronic charge, I = current density, ϵ/K = 11600°C/volt). The slope gives the apparent emitter work function, ϕ_E, and the constant A in Richardson's equation can be calculated and are shown in the figures. The values of ϕ are not very different, but the A's vary considerably. It was found at the end of the experiments that UC was evaporated to a considerable degree and this increased the work functions at the later experiments.

Table XII gives some significant values as: current density (I), cesium mean free path (λ), cesium pressure, cesium density (N_s), power maximum (PM), and voltage at PM (V_{PM}), ϕ_E, and A. An estimate of the maximum electron density N_e was made under the assumption that the cell is operated at $V = \phi_E - \phi_C$, (ϕ_C = collector work function and ϕ_E = emitter work function) and the electrons have only their thermal velocity:

$$V_M = \sqrt{2KT/HM} \quad , \quad \text{or } I/V = N_e \quad .$$

Scattering is neglected for large λ's, and so is the effect of plasma sheaths. If the cell is operated at $V < (\phi_E - \phi_C)$, the motive force is larger than zero, the electron velocity is more than V_M, and therefore the electron density per ampere is much lower. In this case, neutralization of space charge will occur for lower cesium-ion densities.

Table XII shows that the cesium densities are too low for high currents at $V = \phi_E - \phi_C$. This agrees with the voltage-current characteristics qualitatively. Tables for higher cesium pressures and other details are being developed.

Table XII Performance Data on Cesium Diode

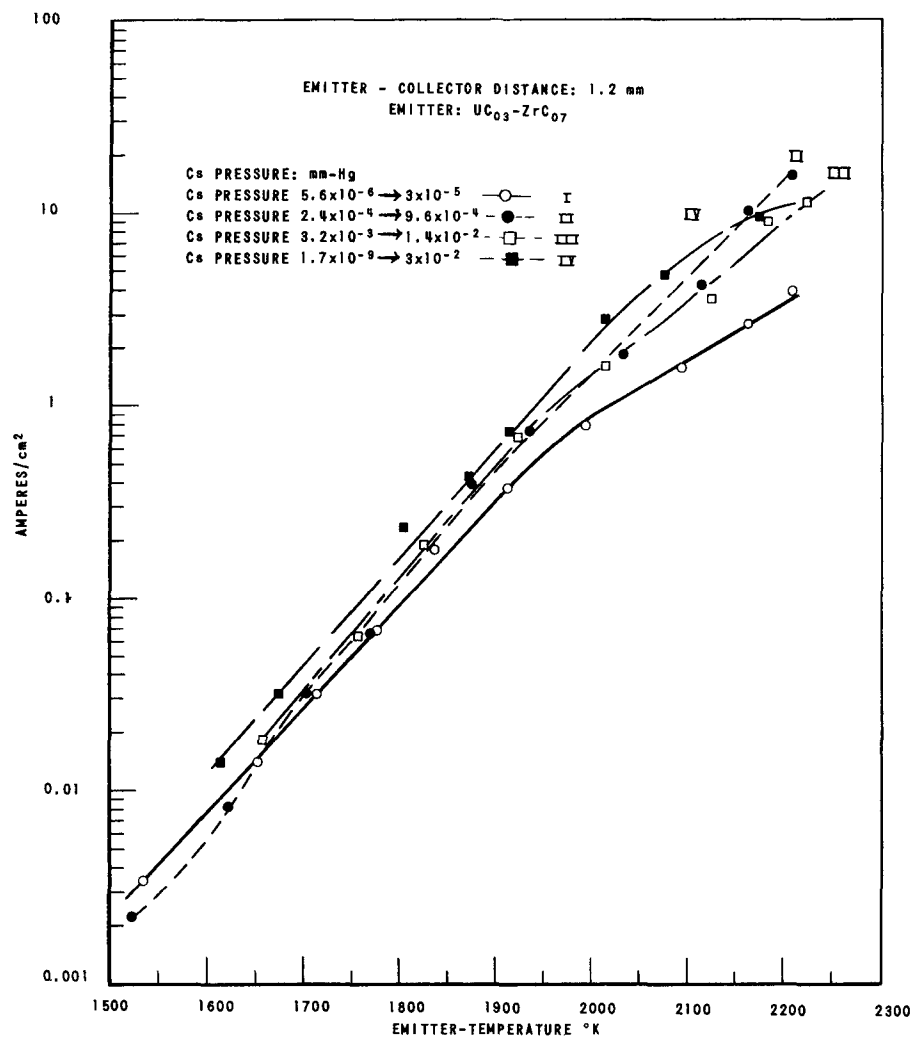| T°K	I/cm² (ma)	λ(MFP) (-cm)	Cs-T°K	Cs-PR (mm-Hg)	N_s(Cs)	N_e	PM (Mw)	V(PM) (volts)	ϕ_E (volts)	Ā (amp/cm²)
1533	3 47	471	312	5 2 x 10⁻⁶	1 06 x 10¹¹	1 78 x 10⁹	3 5	1 5	3 03	9 2
1653	14 2	425	316	9 0 x 10⁻⁶	1 17 x 10¹¹	7 1 x 10⁹	19 0	1 75	See Fig 2	
1713	34 0	425	316	9 0 x 10⁻⁶	1 17 x 10¹¹	1 66 x 10⁹	55 0	2 00		
1778	69 6	425	316	9 0 x 10⁻⁶	1 17 x 10¹¹	3 5 x 10¹⁰	135 0	2 00		
1838	174 0	236	322	1 3 x 10⁻⁵	2 11 x 10¹¹	8 2 x 10¹⁰	300	2 00		
1913	364 0	236	322	1 3 x 10⁻⁵	2 11 x 10¹¹	1 68 x 10¹¹	600 (watts)	2 00		
1993	790 0	160	326	1 8 x 10⁻⁵	3 25 x 10¹¹	3 55 x 10¹¹	1 02	1 75		
2093	1550	160	326	3 10⁻⁵	7 6 x 10¹¹	1 12 x 10¹²	2 25	1 50		
2243	3 95	51 6	337	3 2 x 10⁻⁵	9 7 x 10¹¹	1 72 x 10¹²	4 00	1 50		

Figure 15

Short Circuit Currents
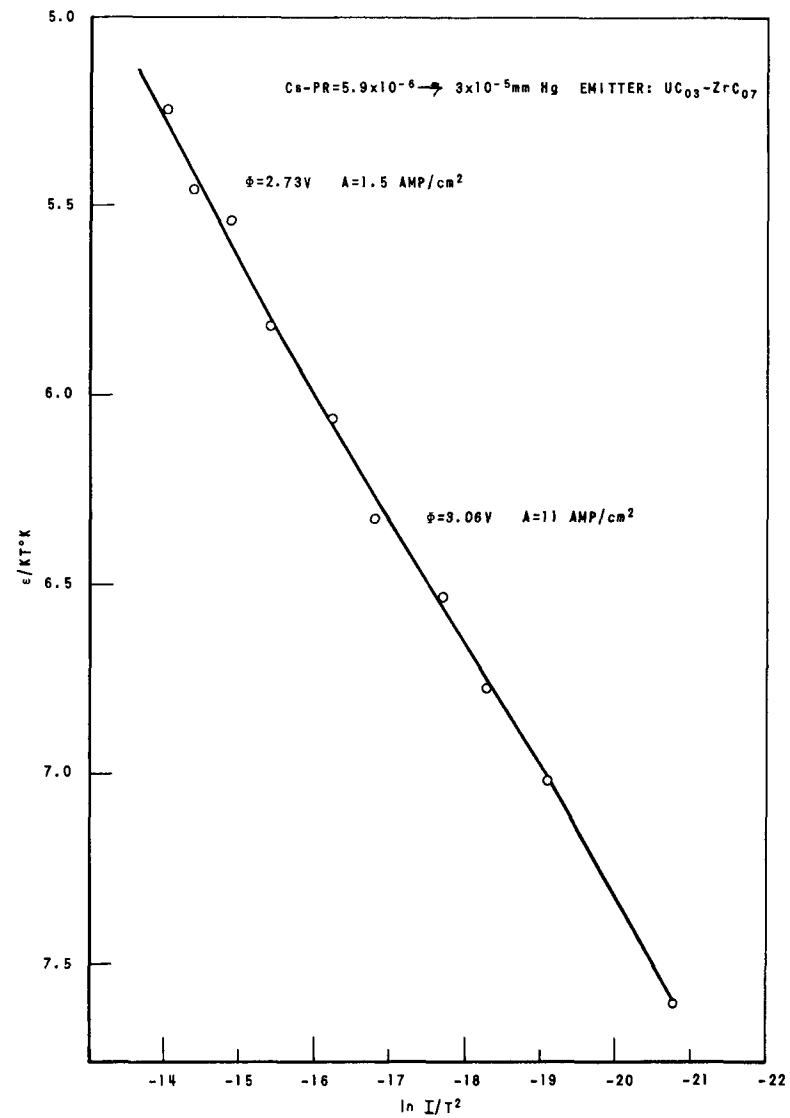
Figure 16

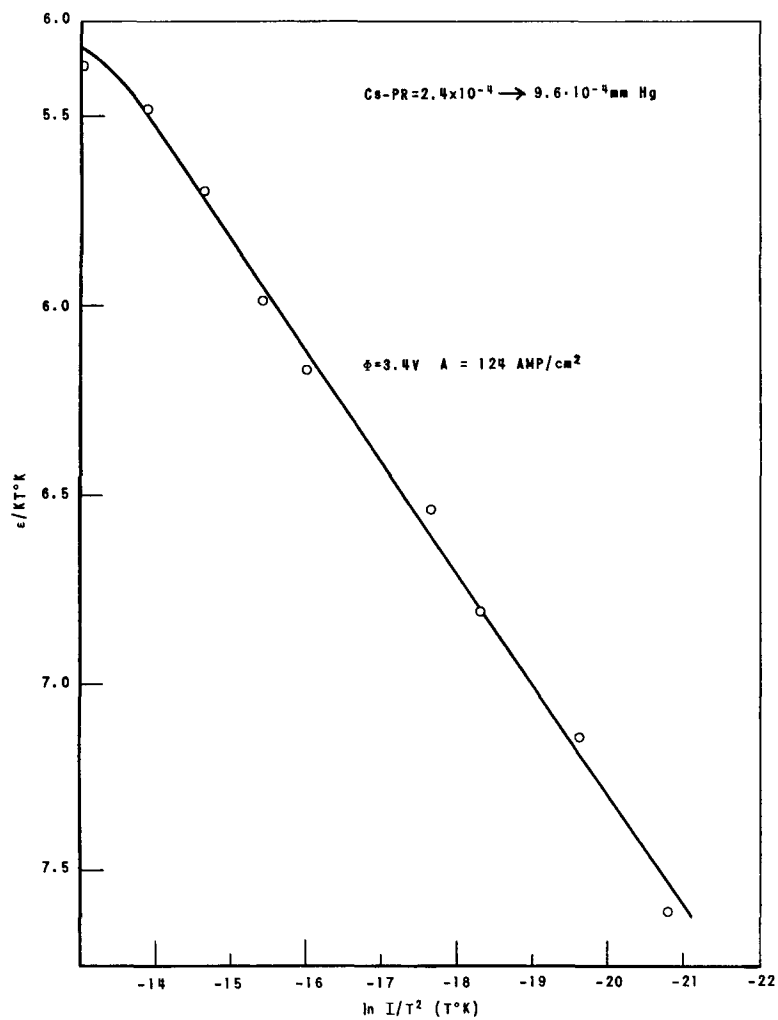**Richardson's Constants:** T^oK: $\epsilon/K = 11600^oK/V$

Figure 17

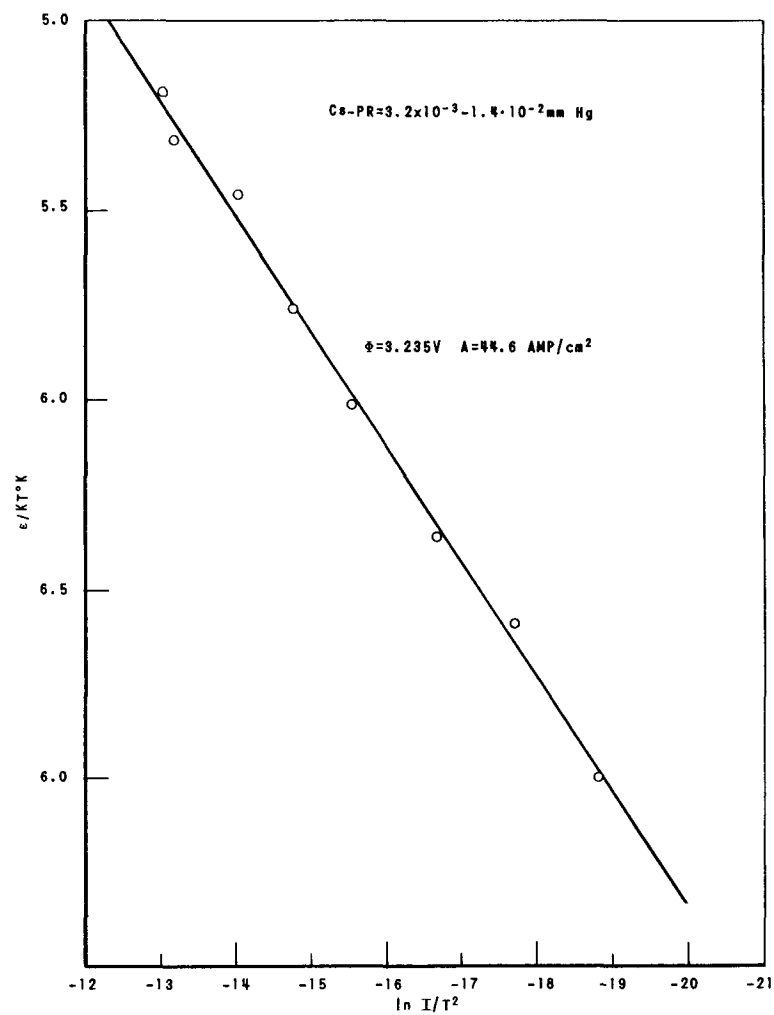Richardson's Constants: $UC_{.03}$-$ZrC_{.07}$ $\epsilon/K = 11600°K/V$

Figure 18

Richardson's Constants, $UC_{.03}$-$ZrC_{.07}$

V. PUBLICATIONS

Papers

THEORY OF AVERAGE NEUTRON REACTION CROSS SECTIONS IN
THE RESONANCE REGION
> P. A. Moldauer
>> Phys. Rev. 123, 968 (1961)

FAST NEUTRON ACTIVATION CROSS SECTION OF Au^{197}
> S. A. Cox
>> Phys. Rev. 122, 1280 (1961)

HEAT TRANSFER IN THERMAL RADIATION ABSORBING AND
SCATTERING MEDIUM
> R. Viskanta and R. J. Grosh
>> International Developments in Heat Transfer, American
>> Society of Mechanical Engineers, New York, N. Y.,
>> Part IV, pp. 820-28 (1961)

FLUORINE BOMB CALORIMETRY: THE HEAT OF FORMATION
OF ZIRCONIUM TETRAFLUORIDE
> E. Greenberg, J. L. Settle, H. M. Feder, and W. N. Hubbard
>> J. Phys. Chem., 65, 1168 (1961)

ANL Reports

ANL-5700   DIFFUSION IN URANIUM, ITS ALLOYS, AND COMPOUNDS
(Part C)   Steven J. Rothman

ANL-6080   SCALE-UP OF HIGH-PURITY URANIUM PRODUCTION.
G. B. O'Keeffe

ANL-6083   METALLURGICAL EVALUATION OF FAILED BORAX-IV
REACTOR FUEL ELEMENT
> C. F. Reinke, L. A. Neimark, R. Carlander
> and J. H. Kittel

ANL-6092   THE DESIGN AND CONSTRUCTION OF THE EBR-II
INITIAL FUEL LOADING FACILITY
> James E. Ayer and Arthur B. Shuck

ANL-6257   STUDIES OF METAL-WATER REACTIONS AT HIGH
TEMPERATURES: I. THE CONDENSER DISCHARGE
EXPERIMENT: PRELIMINARY RESULTS WITH
ZIRCONIUM
> L. Baker, Jr., R. L. Warchal, R. C. Vogel and
> M. Kilpatrick.

ANL-6320   THE DIFFUSION OF CHROMIUM IN GAMMA URANIUM
           S. J. Rothman

ANL-6322   THE FLUID-BED CALCINATION OF RADIOACTIVE
           WASTE
           J. W. Loeding, E. L. Carls, L. J. Anastasia,
           and A. A. Jonke

ANL-6333   CHEMICAL ENGINEERING DIVISION SUMMARY REPORT
           January, February, March, 1961

ANL-6337   CRITICAL STUDIES OF A DILUTE OXIDE FAST
           REACTOR CORE (ZPR-III Assembly 30).
           P. I. Amundson, A. L. Hess, W. P. Keeney,
           J. K. Long, and R. L. McVean

ANL-6340   PREPARATION OF HIGH-DENSITY, SPHERICAL
           THORIUM OXIDE PARTICLES WITH UP TO 10 ATOM
           PER CENT URANIUM
           C. E. Crouthamel, W. G. Knapp, S. B. Skladzien
           and J. W. Loeding

ANL-6346   SYMPOSIUM ON PHYSICS AND NONDESTRUCTIVE
           TESTING
           Held at Argonne National Laboratory October 4
           and 5, 1960

ANL-6357   CRITICAL EXPERIMENTS FOR THE PRELIMINARY
           DESIGN OF THE ARGONNE HIGH FLUX REACTOR
           J. W. L. deVilliers, Editor

ANL-6366   SOME HEAT TRANSFER AND FLUID FLOW
           CONSIDERATIONS FOR A PACKED-BED FUEL
           ELEMENT
           R. Viskanta